AD-A285 808

‖‖‖‖‖‖‖‖‖‖‖‖‖‖‖‖

RL-TR-94-171
Final Technical Report
September 1994

HIGH POWER JOSEPHSON EFFECT SOURCES

State University of New York (SUNY)

DTIC
ELECTE
OCT 3 1 1994
G D

APPROVED FOR PUBLIC RELEASE; DISTRIBUTION UNLIMITED.
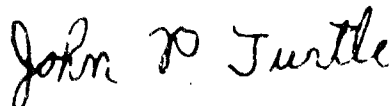
94-33537

‖‖‖‖‖‖‖‖‖‖‖‖‖‖‖‖

Rome Laboratory
Air Force Materiel Command
Griffiss Air Force Base, New York

9410 27 016

This report has been reviewed by the Rome Laboratory Public Affairs Office (PA) and is releasable to the National Technical Information Service (NTIS). At NTIS it will be releasable to the general public, including foreign nations.
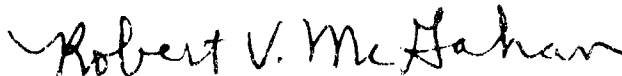
RL-TR-94-171 has been reviewed and is approved for publication.

APPROVED: *John P Turtle*

JOHN P. TURTLE
Project Engineer

FOR THE COMMANDER: *Robert V. McGahan*

ROBERT V. McGAHAN
Acting Director
Electromagnetics & Reliability Directorate

HIGH POWER JOSEPHSON EFFECT SOURCES

James Lukens

Accesion For		
NTIS CRA&I		☒
DTIC TAB		☐
Unannounced		☐
Justification		
By		
Distribution /		
Availability Codes		
Dist	Avail and / or Special	
A-1		

High Power Josephson Effect Sources

Final report on contract # F1962890K0033

The goals of this contract were the development and demonstration of the technologies needed for submillimeter wave sources, based on arrays of Josephson junctions, with power levels above one milliwatt. As a demonstration of this technology it was planned to build a source with about $100\,\mu W$ of power. These goals required several advances in fabrication technology and design concepts.

High power requires that the I_c of the junctions have a value of tens of milliamps. Achieving this while keeping the junction size small enough to avoid flux flow instabilities requires values of J_c approaching $100\,kA/cm^2$. Near the start of this contract we demonstrated the ability to fabricate $Nb/AlO_x/Nb$ trilayers having this range of J_cs and to use these trilayers as part of a complete circuit fabrication technology to make sources using parallel biased junctions having power levels in the $1\,\mu W$ range. This work was presented at the 1990 Applied Superconductivity conference [1] and is described in detail in appendix A.

The array design used in our sources incorporates the junctions in a long niobium microstrip. At frequencies approaching the gap, the losses in this microstrip become significant. An accurate method of measuring these losses in the submillimeter wave range is needed to measure the loss in Nb and other potential stripline material as part of materials fabrication development. Also an accurate measure of the loss is needed in assessing the operation of the array source in order to compare the measured power from the source with that predicted. Such a technique was developed as part of this contract. Here single junctions were incorporated in series with a microstrip resonator made of the material whose loss was to be measured. The junction, which was resistively shunted, acted as both the generator and detector of the submillimeter wave radiation in the microstrip. The amplitude and frequency of the resonance can be determined from the perturbation to the junction's I-V curve. This gives both the real and imaginary parts of the microstrip impedance. These results were published in 1991 [2] and appear in detail in appendix B.

In work under previous contracts and that of Ref. [1], junctions of the oscillator array were placed as wavelength intervals along the microstrip. This "quasi-lumped" design preserved the correct phase relationship among the junctions to ensure stable in-

1

phase locking. However, the large amount of microstrip required would be both too lossy and take up too much space for higher power arrays. As a result of simulations, it was found that groups of junctions covering about 1/4 wavelength could be placed at each half wavelength interval. A small "distributed" array based on this design was fabricated and tested. It showed fully coherent operation, demonstrating that the concept worked as predicted. These results were presented at the 1992 Applied Superconductivity Conference [3] and are described in detail in appendix C.

An important feature of any source is its linewidth. Theoretical analysis indicated that the contemplated high power submillimeter wave sources would have linewidths of around 10 kHz. which is sufficiently narrow for a wide range of applications. These theories had. however. only been tested in lumped arrays in the microwave range since the submillimeter wave sources used on-chip detectors. Work under this contract was therefore carried out to directly measure the linewidth of the array described above (App. C). Two distributed arrays of 10 junctions each. along with an SIS mixer. were fabricated on a single chip forming a combined source-receiver. The mixing product. with an IF of about 10 GHz. was coupled out of the cryostat to a spectrum analyzer. The linewidth was measured as a function of temperature from 1.5 to 4.2 K and found to be within 50% of the theoretical prediction. This result. which was published in 1993 [4] and is described in detail in appendix D. gives strong support to the analysis used to predict the linewidth anticipated from the proposed high power arrays.

Arrays with more that 1 mW of power would contain thousands of junctions each requiring a bias current of tens of milliamps. For the arrays described above. the junctions were biased in parallel so that. for an N junctions array. the bias current would be N times the bias current of a single junction. This arrangement was clearly impractical for very large arrays although it had the advantage of permitting a greater scatter in the junction parameters i. e. I_c and R. An important part of this contact was. therefore. the demonstration that successful operation could be achieved in arrays in which the junctions were biased in series so the total bias current was equal to that of a single junction. We designed such an array. based on the quasi-lumped design. which was fabricated at IBM using the newly developed PARTS technology. Since this array was a small part of a much larger wafer. the values of J_c and R were dictated by the requirements of other circuits and were far from optimal for our sources so that we were only able to design for a power level of 1 μW. The resulting 100 junction array. however. worked perfectly delivering the 1 μW of power to a 50 Ω load on-chip at

300 GHz. This was the first demonstration that the series biased design would in fact perform as predicted. These results were presented at the 1992 Applied Superconductivity Conference [5] and are described in detail in appendix E.

The final phase of our work under this contract was to attempt to combine these various developments to demonstrate a submillimeter wave source with $100\,\mu$W of power. This 500 junction source was designed using the distributed array concept demonstrated above (App. C). It was also fabricated at IBM using the PARTS process--in fact it was the very last circuit fabricated before the line was shut down as part of the IBM retrenchment. This time, however, we were able to include the source as part of a wafer with design parameter much closer to the ideal. The resulting source again operated as predicted. A maximum power of $47\,\mu$W was delivered to a $68\,\Omega$ load on-chip at 394 GHz with as much as $10\,\mu$W (still higher than any other report for a Josephson effect source) observed at 500 GHz. The factor of two difference between the designed and measured power is accounted for since the actual values of J_c and R_n for the fabricated wafer differed somewhat from those expected. Using the measured junction parameters, the observed power demonstrated fully coherent operation of the source so we declare the test to be a success. Various aspects of this work were presented at the 1993 Terahertz Technology Conference at UCLA [6] and at the 1993 ISEC in Boulder [7] (appendixes F and G respectively) and have recently been published in Applied Physics Letters [8]. This work is presented in detail in App. H.

Two Ph. D. theses resulted from work under this contract: "High Frequency Wave Sources Using Josephson Junction Arrays" by Kelin Wan in 1991 and "Development and Application of Josephson Junctions as Submillimeter Wave Sources" by Baokang Bi in 1993.

References

1. K. Wan, B. Bi, A.K. Jain, L.A. Fetter, S. Han, W.H. Mallison, and J.E. Lukens, "Refractory Submillimeter Josephson Effect Sources", *IEEE Trans. Magn.*, Vol. 27, No. 2, March 1991.

2. B. Bi, K. Wan, W. Zhang, S. Han, and J.E. Lukens, "Josephson-Junction Driven Submillimeter Wave Microstrip Resonator", *IEEE Trans. Appl. Supercon.*, Vol. 1, No. 4, December, 1991.

3. B. Bi, S. Han, J.E. Lukens, and K. Wan, "Distributed Josephson Junction Arrays as Local Oscillators", *IEEE Trans. Appl. Supercon.*, Vol. 3, No. 1, March 1993.

4. B. Bi, S. Han, and J.E. Lukens, "Radiation Linewidth of Phase-Locked Distributed Array in the Submillimeter Wave Range", *Appl. Phys. Lett.*, **62** (22), 31 May 1993.

5. S. Han, A.H. Worsham, and J.E. Lukens, "Complete Phase-Locking in a One-Dimensional Series Biased Josephson-Junction Array", *IEEE Trans. Appl. Supercon.*, Vol. 3, No. 1, March 1993.

6. S. Han, B. Bi, W. Zhang, A.H. Worsham, and J.E. Lukens, "High Power Submillimeter Wave Source using Series Biased Linear Josephson Effect Array", presented at the Fourth International Symposium on Space-Terahertz Technology, UCLA, Los Angeles, March 30 - April 1, 1993.

7. S. Han, B. Bi, W. Zhang, and J.E. Lukens, "High Power Submillimeter Radiation from Distributed 1D Josephson Junction Arrays", Proceedings of August, 1993 ISEC Conference.

8. S. Han, B. Bi, W. Zhang, and J.E. Lukens, "Demonstration of Josephson Effect Submillimeter Wave Sources with Increased Power", *Appl. Phys. Lett.*, (to be published).

REFRACTORY SUBMILLIMETER JOSEPHSON EFFECT SOURCES

K. Wan, B. Bi, A.K. Jain, L.A. Fetter, S. Han, W.H. Mallison, and J.E. Lukens

Department of Physics
State University of New York at Stony Brook
Stony Brook. New York 11794

ABSTRACT

Niobium Josephson effect array oscillators have been fabricated and tested. These devices deliver about 1 μW of power, in the submillimeter wave range, to 20–60 Ω load resistors. The present upper frequency limit of about 500 GHz appears to be set by losses in the superconducting microstrip. Data on the submillimeter wave surface impedance of the niobium microstrip and details of the trilayer junction processing, which gives value of V_m at 2K up to 800 mV, will be presented.

INTRODUCTION

The interest in submillimeter wave generation using Josephson junctions and Josephson junction arrays has increased in the past few years because of the possibility of using them as local oscillators for SIS mixers, in communication, and radio–astronomical observation, etc., due to the scarcity of other solid state source in this frequency range.[1-4] A Josephson junction is a voltage control oscillator (VCO) with the potential for wide tunability and a fast tuning rate. Three types of Josephson effect oscillators have been demonstrated , namely, the resonant fluxon oscillator[4], the flux flow oscillator[5], and small junction arrays.[5-6] The first two types use long Josephson junctions with the junction dimension much larger than the Josephson penetration depth. In this paper, we will focus on the small junction arrays.

To overcome the disadvantages of a single junction source, such as low impedance, low output power level, and large linewidth, an array having a large number (N) of junctions , all of which are phase–locked, is employed.[7] The output power level of such an array into a matched load increases as N , while the linewidth of the radiation emitted from array decreases at least as 1/N. To treat the array as a lumped circuit, all of the junctions in the array should be placed within about one eighth of a wavelength. Thus , the number of junctions is limited by the minimum spacing between junctions (about 10 μm) to substantially less than the optimum number of junctions. To circumvent this problem, the concept of a distributed array was introduced.[8-9] Here all junctions are placed one wavelength apart so that, at the operating frequency, the array looks like a lumped circuit. Previously[8-9], we have demonstrated that distributed arrays of Josephson junctions having 40 junctions could deliver 1–7 μW of power onto 20–100 Ω load resistors in the frequency range of 350 GHz to 450 GHz. The upper limit was set by the onset of the large losses in the lead alloy superconducting microstrip. Those arrays were made of Cu–shunted lead alloy tunnel junctions and suffered from the usual problems of

non–uniformity and cyclability characteristic of this technology. In this paper, we report our recent results on similar arrays with Au–shunted Nb/AlOx/Nb junctions , along with the fabrication details and characteristics of the all refractory Nb/AlOx/Nb junctions. Measurements on the surface impedance of the niobium films , using a resonator driven by a resistively shunted Josephson junction source ,are also discussed.

Nb/AlOx/Nb TUNNEL JUNCTIONS

1. Preparation

Junctions were fabricated as outlined below using the very successful niobium trilayer technology (with some local variations) which has been developed extensively during the last decade.[10-14]

The system used for the Nb/AlOx/Nb deposition in the present work consisted of multiple sources including a DC magnetron sputtering gun for Nb deposition and a RF inverted cylindrical sputtering gun for Al deposition. The system was cryopumped, having a base pressure below 2×10^{-7} Torr. The samples were mounted on a water cooled, rotating stage which could be moved over the various sources. The distance between the sample and the target was approximately 5 inches. This rather large spacing was used ,along with cooling water, to ensure the substrate temperature did not rise during the deposition and also to reduce the stress in the films. We found that preventing substrate heating during deposition was crucial to obtain high quality junctions.

The Nb/AlOx/Nb trilayer structure was patterned by means of lift–off using a PMMA–Al–PMMA tri–level mask[8] rather than the more conventional method of etching a uniformly coated substrate. The lift–off method kept the film area small, reducing the stress in the film. This was specially important for high quality small area junctions. The tri–level mask, instead of single level mask, provided a better tapered edge profile than the single level mask.

The Nb/AlOx/Nb trilayer structure was made by sequential deposition in the same chamber. The Nb base electrode was about 1000 Å. The Al varied from 10 Å to 400 Å . And the Nb counter electrode was about 600 Å.

Evaporation rates for niobium and aluminum were 7–8 Å/sec and 2.5–3 Å/sec, respectively. The tunnel barrier was formed by thermal oxidation of the Al. Several means of oxidation, including flowing oxygen gas controlled by mass flow controller, oxygen plasma, and 10 % of O_2 mixed with 90 % of Ar), were tried. It was found that the partial pressure of oxygen determines the oxide thickness if the oxidation time is kept constant. To vary the critical current density, the pressure of the oxygen was fixed at 5 mTorr and the oxidation time was varied from several minutes up to one hour. This gave critical current densities varying, as shown in Fig.1a, from several hundred to about 50 kA/cm², where the gap voltage of the junction was reduced to about 2.5 mV
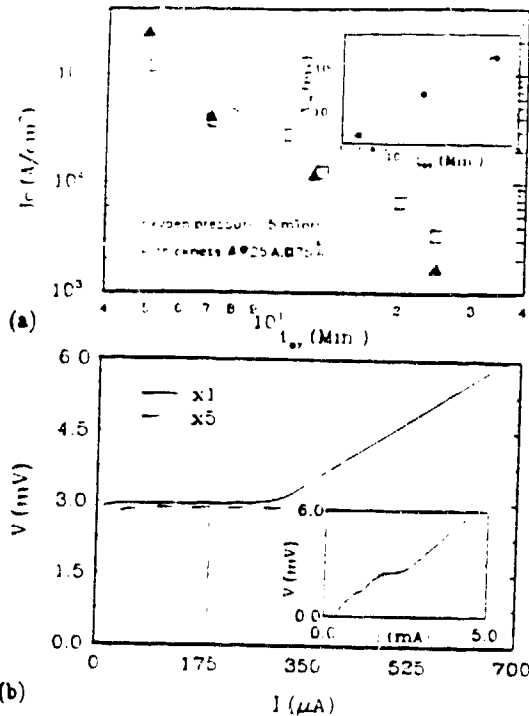
(a)

(b)

Fig.1. (a) J_c vs. oxidation time,t_{ox}, the insert shows the variation of V_m with t_{ox}; (b) I–V characteristic of a high quality junction with V_m=800 mV; the insert shows the I–V characteristic of junction with high critical current density showing the gap voltage above 2.5 mV.

The pattern of the junction counter electrode was defined by electron beam lithography using a single layer *PMMA* mask with a thickness from 5000 $\overset{\circ}{A}$ to 1 μm, depending on the size of the junction needed. The sample was etched by reactive ion etching (RIE) with CF_4 gas mixed with 15 % of oxygen. 1200 $\overset{\circ}{A}$ of SiO was then deposited through the same mask to form an insulating layer, isolating the counter electrode. During the SiO deposition, the samples were tilted about 20 degrees and rotated so that the edges of the junction counter electrode could be fully covered and a uniform SiO layer formed. A niobium wiring layer was deposited at the same rate as the Nb for the trilayer. Before the wiring deposition, the surface of the counter electrode was cleaned by a RF Ar plasma for 5–7 minutes to remove the Nb oxide.

2. Characterization

The I–V characteristics of the Nb/AlOx/Nb junctions show that the junctions can be of high quality including high V_m, high gap voltage, and a narrow gap transition width. Fig.1b shows the I–V curve of a junction with the optimized fabrication parameter using 15 $\overset{\circ}{A}$ Al and oxidation time of 30 minutes. This gave a V_m of about 800 mV and J_c of 1500 A/cm² at 2 K. The insert of Fig.1b shows the I–V curve for a junction with high critical current density (40 kA/cm²). Although the junction has large subgap leakage, its gap is still above 2.5 mV. Junctions with high critical current density are most desirable for Josephson effect oscillators, while the leakage is not important since the junctions are to be resistively shunted in any case.

Although several tens of $\overset{\circ}{A}$ of Al were generally used to make sure the niobium surface was well covered by Al, it had

been shown by X–ray photoemission spectroscopy [12], and anodization spectroscopy [13], that only part of the Al, i.e., about 9–10 $\overset{\circ}{A}$, is oxidized. The extra layer of unoxidized Al can cause a reduction in the junction quality.[10-11] To examine this, the thickness of Al was varied systematically and the dependence of the junction quality, V_m, on the thickness of Al was measured (Fig. 2). The junction quality, as measured both by V_m and the sharpness of the gap, is a maximum for 15 $\overset{\circ}{A}$ of Al, decreasing steadily for both greater and lesser thicknesses. These results are consistent with those obtained by Huggins and Gurvitch.[10]
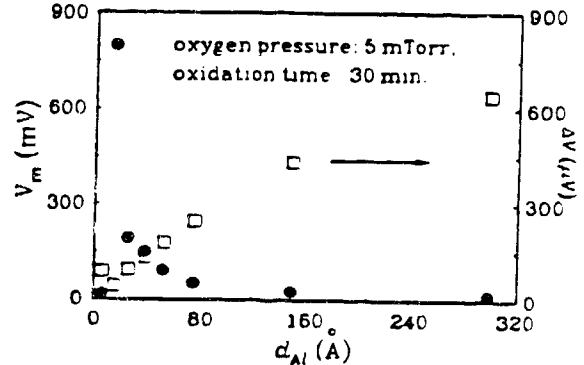

Fig.2. Dependence of the junction quality parameter, V_m, and the transition width of the gap, ΔV,measured at 2K, on the Al thickness.

For use in Josephson junction array oscillators, the junctions are required to have a small β_c ($\beta_c=2\pi C_L R_j^2/\phi_0$) and an I–V characteristic that is non hysteretic. This was achieved using a gold shunt resistor with a 30 to 50 $\overset{\circ}{A}$ Cr underlayer for adhesion, as shown schematically in Fig.3a
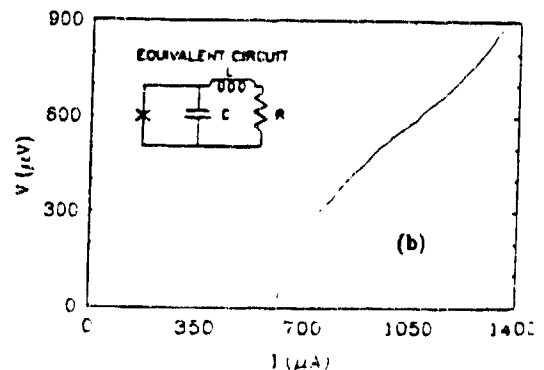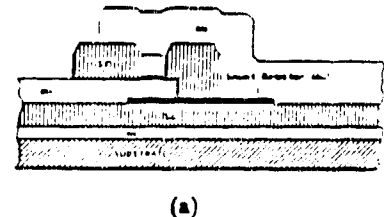

(a)

(b)

Fig.3. (a) Schematic of the Au–shunted Nb/AlOx/Nb junction; (b) I–V curve of the Au–shunted Nb junction, the insert is the equivalent circuit of the junction.

Typically, 300 Å of Au was used, giving a resistance about 1 Ω per square. Fig.3b also gives the I-V characteristics of the Au-shunted Nb/AlOx/Nb junction along with its equivalent circuit.

The junctions used in the submillimeter wave generator are 2x3 μm^2 shunted by an approximately 2 μm long resistor. The critical currents of the junctions vary from 0.5 mA to 1 mA. The specific capacitance, c, of the junctions was determined from the zero field step (ZFS), giving $c \simeq 40$ fF/μm^2. The inductance of the junction shunt resistor loop was estimated to be about L = 0.1 pH. These parameters are small enough for stable operation of the submillimeter wave generator (i.e., β_c, $\beta_f = 2\pi LI_c/\phi_0 << 1$).

Nb/AlOx/Nb JUNCTION ARRAYS

The design of Nb/AlOx/Nb junction array, shown schematically in Fig. 4a, is similar to that of the lead alloy junction arrays, which were discussed in detail in our previous works.[8-9] Because of the non-uniformity of the junction critical current and the shunt resistance (about 10%), a parallel biasing scheme, which compensates, to the first order, for this variation, was still used. All of the junctions are spaced to be one wavelength apart (about 350 μm) at 350 GHz. A resistor (about 20 Ω) is placed at one end of the array to simulate the load. The rf current flowing through the load resistor is monitored by a detector Josephson junction placed at one end of the load resistor. The array and load are rf grounded by using a quarter-wavelength microstrip. Direct grounding (microstrip line shorted to the ground plane) has also been tried with similar results.
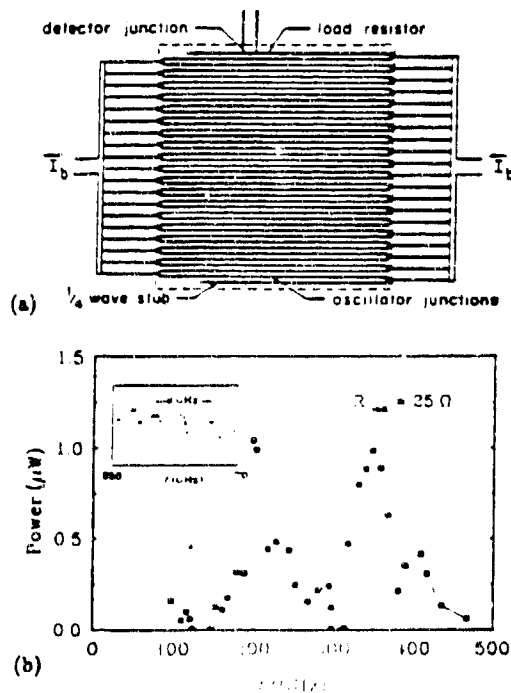
(a)

detector junction — load resistor

$\overline{I}_b$ ... $\overline{I}_b$

¼ wave stub — oscillator junctions

(b)

Power (μW)

$R_{\text{load}} = 25 \Omega$

0   100   200   300   400   500

FREQ (GHz)

Fig.4.(a) Schematic of the parallel biased distributed array. The junctions (x) are placed at 350 μm intervals along the serpentine microstrip. The load resistor and detector junction are shown in the upper left. The dashed lines show the extent of the ground plane under the microstrip. (b) Power vs frequency; the insert is the expansion near 260 GHz, showing a periodicity of about 4.5 GHz.

The critical current and the shunted resistance of the junctions used for these arrays were 0.5-1 mA and 0.5 to 0.7 Ω, respectively, giving the I_cR_i product of about 500 μV, and $\beta_c << 1$, the I-V curve of the array is non hysteretic. The arrays using Nb/AlOx/Nb junctions generally operate over a much wider frequency range, from 100 GHz to above 500 GHz, and exhibited increased cyclibility and parameter uniformity. The arrays can deliver a power of about 1 μW to 20-60 Ω load resistors as seen in Fig. 4b, showing the power to the load vs. frequency as the array bias is varied. The power level was determined by using the Josephson junction detector by measuring the amplitude of the first Shapiro step.[8-9] The insert of Fig. 4b shows the details of this power variation near 260 GHz. One can see that the power varies with a periodicity of about 4.5 GHz which corresponds to $\bar{c}/2l_t$, where $\bar{c}$ and l_t are the phase velocity and the total length of the array. As can be seen, appreciable power is obtained from the array, not only at designed frequency ν_0 and $\nu_0/2$, (where the junctions are spaced by λ and $\lambda/2$, respectively) but also over a wide range of frequencies satisfying $f_0 = n \bar{c}/2l_t$ (n an integer). A theory for this broad band operation has yet to be worked out.

We have not yet made a direct measurement of the linewidth of the radiation from this array. The RSJ analysis, which agrees within a factor of two with the measured linewidth for parallel arrays in the microwave range[11], was used to estimate the linewidth, for these submillimeter arrays. The linewidth of the radiation at ν_0 is thus estimated to be 60 KHz at 2 K, and 130 KHz at 4.2 K, respectively from the measured differential resistance based on this lumped circuit analysis.
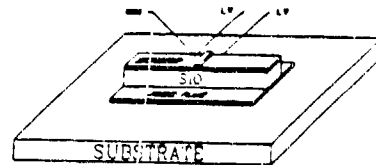
Fig.5. Schematic of the resonator driven by a Josephson junction source as used for surface impedance measurements.

SURFACE RESISTANCE OF THE MICROSTRIP

In order to measure the phase velocity and loss of the superconducting microstrip in the submillimeter wave range, a microstrip resonator which uses a Josephson junction as both the source and detector has been developed. The schematic of this resonator is shown in Fig.5. Our approach differs somewhat from previous measurements[10-17] of this type in that a resistively shunted junction has been used in the resonator. In the absence of rf currents flowing in the resonator, the I-V curve of the junction is given analytically by the well known RSJ model. The bias leads, which are placed next to the junction act as a high impedance transmission line, which if properly terminated, simply causes a slight shift in the shunt resistance.

The rf currents which flow in the microstrip when the wavelength $\lambda = 2 l$ where l is the length of the resonator, act as a perturbation on the RSJ solution. The junction's characteristic frequency, given by its I_cR_i product, is selected to be near or below the frequencies of interest. For these conditions, the well established perturbation approach agrees very well with direct computer simulations. The junction's response is thus well characterized and easy to analyze. The mixing of Josephson oscillations in the junction with the rf microstrip currents produces a shift in the bias current required for a given operating frequency or voltage. This shift δI is given by $\delta I = $ const $Re(1/Z)$ where Z is the rf loop impedance of the structure shown in Fig 5. Thus the difference

between the junction's bias currents with and without the microstrip resonance is just a resonant peak as shown in Fig.6. Here the data with the best fit RSJ background subtracted are shown as points, while the best fit to the theory is the solid line. The resonant frequency (194 GHz) gives the phase velocity
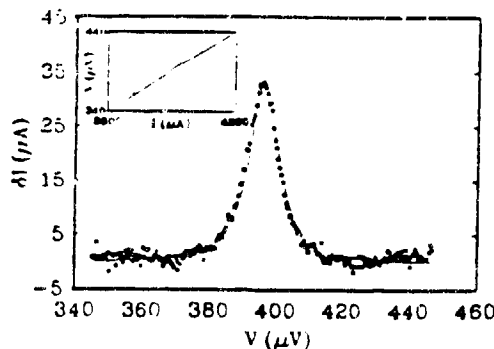

Fig.6. Detail of resonance peak δI (■) with the best theoretical fit (—), the insert is the I–V curve of the junction in the resonator.

$V_p = 0.4c$ and the Q ($\approx$ 50) gives the loss in the microstrip. For the microstrip dimensions of 300 μm long by 10 μm wide, this Q implies a surface resistance of 3 mΩ for the line at 4.2K.

CONCLUSION

We have discussed the fabrication and characterization of Nb/AlOx/Nb junctions having V_g of up to 800mV at 2K Arrays using Nb/AlOx/Nb junctions have been fabricated and tested. These arrays, which delivered about 1 μW of power to 20–60 Ω load resistors operated over a wide frequency range, from 100 GHz to 500 GHz, and exhibited improved cyclibility and parameter uniformity compared to arrays using lead alloy junctions. The surface impedance in the submillimeter wave range was measured using a microstrip resonator driven by a Josephson junction, giving $R_s \approx$ 3 mΩ at 4.2K

ACKNOWLEDGEMENT

REFERENCES

1 K.K. Likharev, Dynamics of Josephson Junctions and Circuits, Gordon and Breach Science Publishers, New York, 1986, Chap.13

2 A.K. Jain, K.K. Likharev, J.E. Lukens and J.E. Sauvageau, "Mutual Phase-locking in Josephson Junction Arrays," Phys. Rep., 109, 309, 1984

3 G.S. Lee and S.E. Schwarz, "Mutual Phase-locking in Series Arrays of Josephson Tunnel Junctions at Millimeter Wave Frequency," J. Appl. Phys.,60, 465, 1986

4 R. Monaco, S. Pagano, and G. Costabile, "Superradiant Emission from an Array of Long Josephson Junctions," Phys. Lett., A131,122,1988.

5 K. Yoshida, J. Qin, and K. Enpuku,"Inductive Coupling of a Flux-Flow Type Josephson Oscillator to a Stripline", IEEE Trans. Magn., MAG-25, 1084, 1989.

6 J.E. Sauvageau, "Phase-locking in Distributed Arrays of Josephson Junctions," Ph.D.dissertation, SUNY at Stony Brook,(unpublished,1987).

7 J.E. Lukens, A.K. Jain, and K. Wan, "Using the Josephson Effect for Millimeter and Submillimeter Wave Generation,"Sensing, Proceeding of NATO Advanced Study Institute on Superconducting Electronics, edited by H. Weinstock and M.Nisenoff, Springer, New York and Heidelberg, 1989.

8 K. Wan, A.K. Jain, and J.E. Lukens, "Submillimeter Wave Generation using Josephson Junction Arrays," IEEE Trans. Magn.,MAG-25, 1076, 1989.

9 K. Wan, A.K. Jain, and J.E. Lukens, "Submillimeter Wave Generation Using Josephson Junction Arrays," Appl. Phys. Lett.,54, 1085, 1989.

10 H.A.Huggins and M.Gurvitch, Preparation and characteristic of Nb/Al-oxide/Nb tunnel junctions",J. Appl. Phys.,57, 2103 (1985).

11 M. Gurvitch, W.A. Washington, and H.A. Huggins, "High Quality Refractory Josephson Tunnel Junction Utilizing Thin Aluminum Layers," Appl. Phys. Lett., 42, 472, 1983.

12 J.Kwo, G.K.Wertheim, M.Gurvitch, and D.M.E.Buchanan,"X-ray Photoemission Spectroscopy Study of Surface Oxidation of Nb/Al Overlay Structures," Appl. Phys. Lett.,40, 675(1982).

13 T. Imamura and S. Hasuo, "Characterization of Nb/AlOx-Al/Nb Structures by Anodization Spectroscopy," IEEE Trans Magn.,MAG-25, 1131, 1989.

14 A.W.Lichtenberger, C.P. McClay, R.J.Mattauch, M.J. Feldman, S-K.Pan, and A.R.Kerr,"Fabrication of Nb/AlOx/Nb Junctions with Extremely Low Leakage Current", IEEE Trans. Magn.,MAG-25, 1247,1989.

15 K. Wan, A.K. Jain, and J.E. Lukens (unpublished).

16 A.D.Smith,B.J.Dalrymple,A.H.Silver,R.W.Simon, and J.F.Burch, "Microstrip Resonances in Superconducting Circuits", IEEE Trans Magn.,MAG-23,796, 1987.

17 A. Larsen, H.D. Jensen, and J Mygind, "Josephson Tunnel Junction Coupled to Superconducting Thin-Film Resonator", LT-19, 1990 (to be published).

Josephson-Junction Driven Submillimeter Wave Microstrip Resonator

Baokang Bi, K. Wan, Wenxing Zhang, Siyuan Han, and James E. Lukens

Abstract —A microstrip resonator driven by a resistively shunted Josephson junction has been used for submillimeter wave surface resistance measurements to about 400 GHz. A simple, analytical analysis of the resonator induced structure in the junction's $I-V$ characteristic gives the resonator surface resistance in the range of 2-160 mΩ with an accuracy of better than 30%.

I. INTRODUCTION

THE DEVELOPMENT of thin film devices in the submillimeter wave range has become an active research area, leading to the need to understand the physical properties, such as the surface resistance and of materials in this frequency range. Below about 200 GHz, resonant cavities coupled to solid state (e.g., Gunn) oscillators are useful for these measurements, while for $f \geq 1$ THz, infrared techniques become available. For intermediate frequencies, due to the lack of suitable sources, surface resistance measurements have proven more difficult. One choice for these frequencies is to use superconducting Josephson junction oscillators. The Josephson junction is a natural voltage controlled oscillator, with an oscillation frequency related to its dc bias voltage by $f = 2eV/h = 483$ GHz mV. For typical junctions (e.g., Nb/AlO$_x$/Nb), oscillations are sustained to over 1 THz. When coupled to a resonant structure, the Josephson junction radiates into the resonator, while the resonator current interacts with the junction. The results of this interaction are reflected in the junction dc $I-V$ curve, which carries the information about the resonator. This phenomenon has been studied theoretically by, e.g., Likharev [1].

There are two useful systems, distinguished by the mode of coupling to the resonator. The first one, which has been widely used, consists of a weakly damped SIS junction coupled to a parallel type of resonator. This system has been used to improve the impedance matching of SIS mixers [2] and to measure the phase velocities of dielectric materials [3], [4]. The second system is made of a highly damped Josephson junction coupled to a series type of resonator. The resonances in this latter system have been experimentally demonstrated by using point contact [5] and microbridge [6] junctions.

In this paper, we report work on developing a resistively shunted Josephson junction (RSJ) driven submillimeter wave

microstrip resonator, as shown in Fig. 1. This enables us to measure both the surface resistance R_s, defined as the resistance per square, and the relative dielectric constant ϵ_r in this frequency range. The interaction of the RSJ with the resonator shows up as a bump (see Fig. 2(c)) on the smooth $I-V$ curve of the unperturbed junction and can easily be calculated by using either numerical analysis or perturbation analysis [7] starting from the analytical RSJ $I-V$ curve. The resonance due to the coupling between the RSJ and the resonator has two main features. The first feature is the center resonant frequency, which depends on the dielectric material used. The second one is the resonant width or Q factor, which is related to the loss in the system. By using the RSJ as both the submillimeter wave source and the detector, both of these two features can be readily obtained from the junctions's dc $I-V$ curve. Therefore, the values of R_s and ϵ_r can be extracted. Other advantages of using the RSJ, such as a smooth $I-V$ background curve and continuously tunable operating frequency are also important considerations for its choice.

II. DEVICE PREPARATION

Fig. 1 shows the structure of the microstrip resonator. A patterned ground plane is deposited first. The supporting SiO dielectric is then thermally evaporated in a chamber with base pressure in the 10^{-7} torr range. Finally, the microstrip transmission line with the RSJ at its center is fabricated. The microstrip transmission line, the SiO dielectric layer, and the ground plane form an open ended microstrip resonator. The materials used for making the resonator are indicated by the notation MS/SiO/GP. Typically, the thickness of SiO dielectric d is 700 nm, and the width of microstrip w is 10 μm. The length of resonator l is determined by the desired frequency and the phase velocity in the dielectric, for example, $l = 200$ μm for a 300-GHz fundamental resonance with thermally evaporated SiO dielectric. The RSJ's used here are mainly Au shunted Nb/AlO$_x$/Nb junctions, using Nb/AlO$_x$/Nb trilayer technology, as given in [8]. Pb-alloy junctions are also used occasionally and are described in [9].

One important design parameter of the RSJ is its $I_c R_j$ product, where I_c is the critical current and R_j is the shunt resistance. The spectrum of Josephson oscillations is rich in higher order harmonics [7] when the bias voltage is low ($V < I_c R_j$). To ensure monochromatic Josephson oscillation, $I_c R_j$ should be smaller than the designed resonant frequency, $I_c R_j < h f_0 / 2 e$. On the other hand, the junction resistance R_j should be kept small for the purposes of both reducing the resonator loss and suppressing the subgap struc-
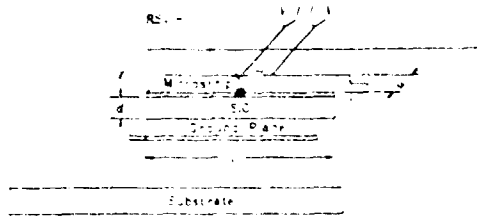
Fig 1   Structure of microstrip resonator RSJ is located at the center of microstrip I-V curve is taken by using 4-terminal measurements
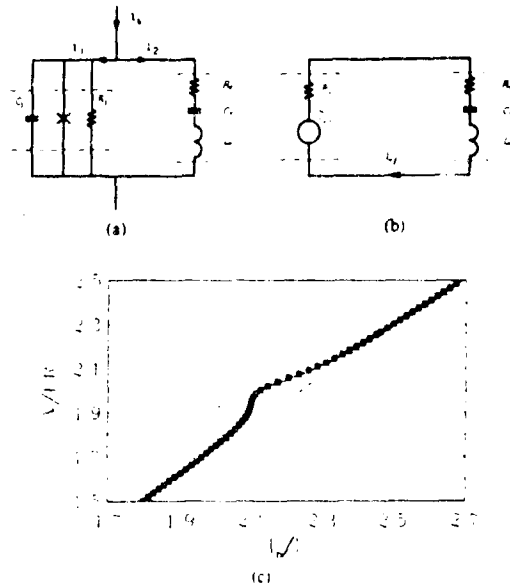

Fig 2.   (a) Equivalent electrical circuit for a junction coupled to a resonator R-L-C series resonant circuit is used to simulate the microstrip resonator for theoretical calculation (b) High frequency equivalent circuit of (a) RSJ is modeled as a RF oscillator with internal source resistance R_j. The oscillator produces a RF current I_{rf} in the loop (c) Comparison of calculated results from numerical analysis (solid line) and perturbation theory (solid square) Unperturbed I-V curve (dash line) is defined as background I-V curve. The bump in the I-V curve is due to the interaction with the resonator.

ture, which is essential to obtaining a smooth background I-V curve. The ground plane is only about 10 μm wider than the microstrip, so that the bias leads, placed close to the RSJ, can come off the ground plane immediately. This reduces the RF leakage through the dc bias leads to a minimum. Table I summarizes the important dimensions and fabrication conditions of the materials used for making the microstrip resonators.

III. ANALYSIS

The microstrip resonator is characterized by the attenuation constant α, the wave number β, and the characteristic impedance Z_0 which is determined by unit length inductance L and capacitance C of the microstrip transmission line, $Z_0 = (L/C)^{1/2}$. The resonator has length l and width w. The thickness of the dielectric is d. Fig. 2(a) shows the equivalent electrical circuit for a RSJ coupled to a resonator.

For simplicity in numerical simulation, the microstrip resonator is replaced with a R_r-L_r-C_r series resonant circuit, where $R_r = \alpha l Z_0$ represents the total loss in the microstrip resonator, and $L_r = lL/2$ and $C_r = 2lC/\pi^2$ are the equivalent inductance and capacitance for the resonator shown in Fig. 1 at the fundamental resonance. The effect of junction shunt capacitance is neglected for our samples, since $\beta_c = 2el_cR_j^2C_j/\hbar < 0.02$. Fig. 2(b) shows the high frequency equivalent circuit [7], where the junction is modeled by a RF oscillator with internal source resistance R_j. The behavior of this RSJ, when coupled to a resonator, can be analyzed in two ways. The fundamental method is by the numerical solution of the set of differential equations describing the circuit. In normalized units, $i = I/I_c$, $v = V/I_cR_j$, $\tau = 2el_cR_jt/\hbar$, these can be written, for the electrical circuit shown in Fig. 2(a), as

$$i_b = i_1(\tau) + i_2(\tau) \tag{1}$$

$$i_1(\tau) = \dot{\varphi}(\tau) + \sin\varphi(\tau) \tag{2}$$

$$\ddot{\varphi}(\tau) = i_2(\tau)r_r + \beta_{lr}\ddot{i}_2(\tau) + \beta_{cr}^{-1}i_2(\tau) \tag{3}$$

where i_b is the dc bias current, $i_1(\tau)$ is the current flowing through the junction, $i_2(\tau)$ is the current in the resonator branch, and $\dot{\varphi}(\tau) = v(\tau)$ is the voltage across the junction. $r_r = R_r/R_j$ is the normalized resistance of the resonant circuit. The capacitance C_r and the inductance L_r of resonant circuit are included in the parameters $\beta_{cr} = 2el_cR_j^2C_r/\hbar$ and $\beta_{lr} = 2el_cL_r/\hbar$. Equation (2) is the dynamic equation for a resistively shunted junction [1], and (3) is the differential equation for the resonant circuit. Equations (1)-(3) are coupled equations and, in general, can only be solved numerically. By taking the time average of $v(\tau)$, the dc I-V curve of the junction is obtained. An alternative and more instructive method for understanding the behavior of the RSJ is perturbation theory [7]. In this theory, the interactions between the RSJ and external radiation are considered as a perturbation to the RSJ I-V curve, which is given analytically by the well-known RSJ model [1]. When biased near the resonance, the junction oscillation produces a RF current I_{rf} in the resonator (see Fig. 2(b)). This RF current in turn mixes with the junction oscillation. The results of this interaction, following from the perturbation theory, are reflected as an effective dc offset i_m in the bias current

$$i_m(v) = \gamma v_m y(v) \tag{4}$$

where $v_m = V_m/I_cR_j$ is the normalized magnitude of Josephson oscillation, γ is the down conversion coefficient of mixing, and $y(v) = R_j$ Re$(1/Z)$ is the real part of normalized admittance for the loop shown in Fig. 2(b). The offset current i_m has been normalized to I_c. Within the resonant

width, both γ and v_m can be treated as constants. When the junction frequency is swept across the resonance, $i_m - v$ has a universal Lorentzian resonant shape with its Q determined only by the loop admittance. The dc I-V curve is, therefore:

$$i(v) = i''(v) - i_m(v). \qquad (5)$$

The first term on the right side $i''(v) = (1 + v^2)^{1/2}$ is the unperturbed RSJ I-V curve, which we call the background I-V curve. The second term on the right side is the perturbative term. I-V curves for identical parameters have been calculated by using both (1)-(3) and (5). As can be seen in Fig. 2(c), the results from these two approaches agree well with each other. Perturbation theory, however, provides simple analytical results for the structure induced on the I-V curve by the resonator, simplifying the data analysis.

For the resonator used, an open ended microstrip transmission line with a junction placed at the center, the loop impedance seen by the oscillator is the sum of source impedance and the transmission line impedance:

$$Z = R_j + 2 Z_0 \coth\left(\frac{l}{2}(\alpha + i\beta)\right) \qquad (6)$$

where Z_0, the characteristic impedance of microstrip line, can be calculated using the equation given by [10]. At resonance, the imaginary part of (6) vanishes, which gives resonant frequencies

$$f_n = \frac{(2n - 1)}{2} \frac{v_p(\epsilon_{\text{eff}})}{l}, \qquad n = 1, 2, \cdots \qquad (7)$$

where l has been taken as the physical length of the resonator since the corrections due to the open ends are calculated to be 0.1%. $v_p(\epsilon_{\text{eff}})$ is the phase velocity, the formulation of which is given in [10] for superconducting microstrip lines. ϵ_{eff} is the effective dielectric constant and is related to the relative dielectric constant ϵ_r by $\epsilon_{\text{eff}} = (1/2)(\epsilon_r + 1) + (1/2)(\epsilon_r - 1)(1 + 12d/w)^{-1/2}$ [11]. The effect of microstrip dispersion on ϵ_r is negligible here. Assuming that there are no other losses, the surface resistances per square are directly related to the attenuation constant α [11] by

$$R_{s1} + R_{s2} = 2\alpha w Z_0 \qquad (8)$$

where R_{s1}, R_{s2} are the surface resistances of the microstrip and the ground plane, respectively. The Q of resonance can be calculated as

$$Q = \frac{\pi}{2} \frac{Z_0}{R_j + \alpha l Z_0}$$

$$= \frac{\pi}{2} \frac{Z_0}{R_j + R_s(l/w)}. \qquad (9)$$

The last equal sign assumes that $R_s = R_{s1} = R_{s2}$ if the microstrip and the ground plane are made of the same materials.

For data analysis, perturbation theory is used. The resonant peak is obtained by subtracting the best fitted background $i''(v)$ from the experimental I-V curve. The attenuation α is then extracted by fitting the resonant peak to (4),

where the loop admittance $y(v)$ is calculated from (6) and γv_m is simply treated as a scaling constant. The surface resistance follows from (8), assuming that there are no other sources of loss in the microstrip.

IV. RESULTS

A typical experimental curve from a Nb/SiO/Nb resonator is shown in Fig. 3 with the junction having $I_c R_j = 153$ V, $R_j = 96$ mΩ, and the microstrip having $l/w = 30$ and $Z_0 = 10$ Ω. The structure appearing on the I-V curve in Fig. 3(a) is due to the resonance from the microstrip resonator. Fig. 3(b) is the resonant peak after the background $i''(v)$ has been removed. The best fit to (4) gives $Q = 54$, $f_0 = 198$ GHz, implying $R_s = 6.1$ mΩ. The effect of thermal noise is negligible for this resonance. A number of samples, made of different materials and with different designed resonant frequencies, have been fabricated and tested. The surface resistance values obtained from those experiments at 4.2K are summarized in Fig. 4(a). For Nb films, the data were collected from several different resonators made with different designed frequencies and most likely having a variation in R_s among them. The solid line is the calculated surface resistance of the Nb microstrip transmission line by using the Mattis-Bardeen theory [12], [13] with a film thickness of $t = 300$ nm, $\sigma(10K) = 2.8 \cdot 10^7 \Omega^{-1} \text{m}^{-1}$, and $2\Delta = 2.6$ mV. Presently, the experimental data cover the frequency range up to 400 GHz. Phase velocities measured from Nb/SiO/Nb microstrip resonators at 4.2 K are plotted in Fig. 4(b). Within this frequency range, v_p is almost constant. By using the average phase velocity, taking $\lambda_{Nb} = 83$ nm [14] and the dielectric thickness $d = 700$ nm, the relative dielectric constant for our thermally evaporated SiO is calculated to be $\epsilon_r = 5.55 \pm 0.14$ which is in good agreement with data published for frequencies under 100 GHz [15]. The solid line in Fig. 4(b) is the phase velocity calculated by taking $\epsilon_r = 5.55$, where the complex conductance from the Mattis-Bardeen theory is used.

V. DISCUSSIONS

The surface resistance values obtained from the previous experiments have been attributed to conductor losses of metal films forming the microstrip resonators. However, other loss mechanisms, such as radiation loss and dielectric loss, also exist in the resonator. Accurate calculation of those losses in our resonator is very difficult, so only estimations will be given. The amount of energy radiated from the open ends depends on the design parameters and operating frequency of the microstrip resonator. The radiation Q factor for a half wavelength resonator, such as ours, has been calculated by Lewin [16]. For $Z_0 = 10$ Ω, $f = 200$ GHz, $d = 700$ nm, and $\epsilon_r = 5.55$, one has $Q_r = 13\,000$. The loss tangent for SiO in the submillimeter wave range at low temperature is not known at present. From the available data at 4.2 K and 30 GHz [17], a value of $\tan\delta_d \sim 10^{-3}$ should be a reasonable estimate for $\tan\delta_d$ at several hundred gigahertz. This gives $Q_d = 1/\tan\delta_d = 1000$. By using (9), the losses from radiation and the dielectric can be expressed in terms of surface resistance. Taking $l/w = 30$, then $R_{rad} = 0.04$ mΩ, $R_d = 0.5$ mΩ. Among R_{rad} and R_d, the dielectric loss R_d
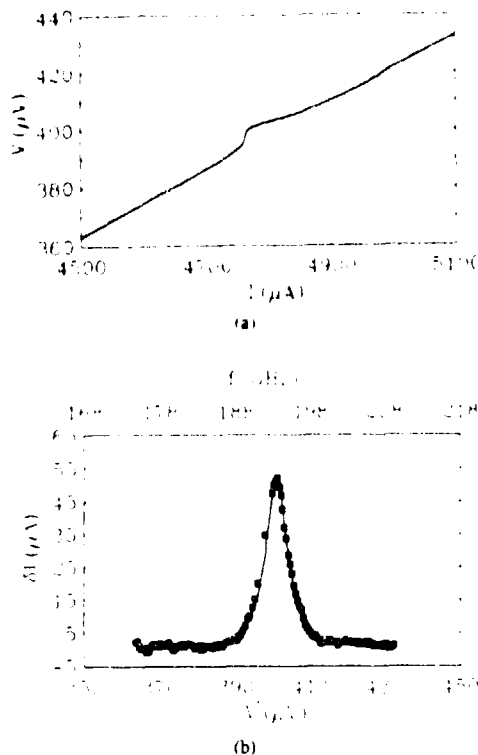
(a)

(b)

Fig 3. (a) Typical experimental I-V curve showing resonance (b) The resonant peak (solid square) from (a) after background is removed Solid line is the best fit to perturbation theory giving $Q = 54$
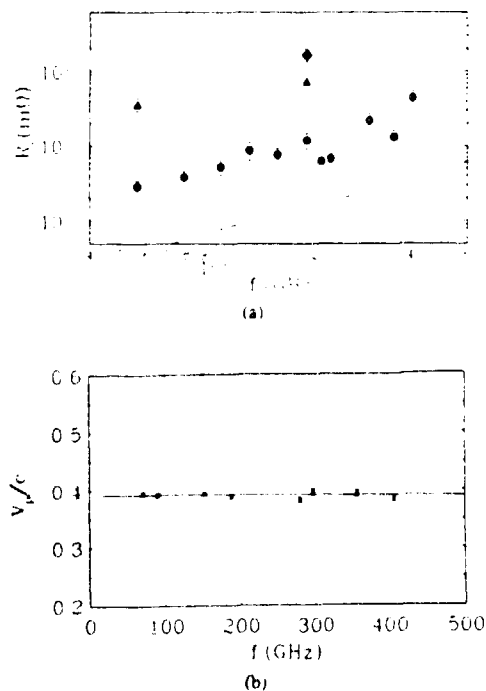

(a)

(b)

Fig 4. (a) Extracted surface resistance values of Au (diamond) from Pb SiO/Au(100 nm), Cu (triangle) from Pb SiO Cu(150 nm), and Nb (circle) from Nb SiO Nb(300 nm) at 4 2K from 50 to 400 GHz Solid line is the surface resistance of Nb microstrip at 4 2K with $2\Delta = 2.6$ mV, calculated by using Mattis-Bardeen theory. (b) Phase velocities (square) measured from Nb SiO Nb microstrip resonators at 4.2K from 50 to 400 GHz Solid line is the phase velocity given by Mattis-Bardeen calculation with $\epsilon_r = 5.55$. Note small curvature.

is the largest, and could be as large as 0 5 mΩ. With those in mind, it is sensible to conclude that the dominant loss in Fig 4(a) comes from the conductor

The smallest surface resistance that can be measured by using this method is limited by the low frequency voltage noise and by the total internal losses including oscillator shunt resistance, dielectric loss, and radiation loss. The total internal loss should be kept as small as possible By using a suspended ground plane, dielectric loss could be reduced to minimum. A smaller shunt resistance $R_j < 0.5R_r$ should also be chosen so that the loss due to the surface resistance always dominates, as shown in Fig. 3.

The upper bound of the measurable surface resistance is primarily determined by how well a broad resonant peak can be recovered from the background I-V. For the resonators made of superconducting materials, when the operating frequency $f > 2\Delta/h$, the surface resistance increases dramatically and the resonance is not detectable. this limits the highest usable frequency, to be about 650 GHz, if Nb is used for the microstrip.

The remaining uncertainties of the surface resistance data can be evaluated from known parameters. The uncertainties of width $\Delta w/w$, and characteristic impedance Z_0 are about 5 and 13%, respectively, as estimated from fabrication control over the microstrip parameters. Errors of $\Delta\alpha/\alpha$ from data fitting are no more than 5% in most cases, giving an overall uncertainty of deduced surface resistance values of about 25%.

A final remark on our experimental results is that the surface resistance values are measured from real devices. which have gone through a series of fabrication steps. Metal thin films may have fine grains, stress, and surface layers, especially for Nb films. All those factors tend to deteriorate the RF properties of thin films. Therefore, the microstrip resonator described here is not an ideal system for measuring the intrinsic losses of conducting thin films unless precautions are taken in preparing and characterizing the thin films, but is suitable for measuring *in situ* physical parameters which are very important for designing practical RF devices like phase-locked submillimeter wave oscillators [7]-[9] and microstrip transmission lines. Placing the films to be measured on a suspended ground plane would also alleviate the problems. Work on this technique is in progress.

VI. CONCLUSIONS

In summary, RSJ driven submillimeter wave microstrip resonators have been developed. The behavior of a RSJ coupled to the microstrip resonator has been well characterized theoretically. The microstrip resonators have been used to measure the submillimeter surface resistance with an accuracy of 25% as well on the dielectric constant up to 400 GHz. This method can be readily extended to a higher frequency range by using superconductors with a larger gap energy 2Δ.

ACKNOWLEDGMENT

REFERENCES

[1] K. K. Likharev. Dynamics of Josephson Junctions and Circuits. Gordon and Breach Science. 1986.

[2] A. V. Raisanen. W. R. McGrath. P. L. Richards and F. L. Lloyd. "Broad-band RF match to a millimeter-wave SIS quasi-particle mixer." IEEE Trans. Microwave Theory Techn., vol. MTT-33, pp. 1495-1500, Dec. 1985.

[3] A. D. Smith. J. A. Carpenter. D. J. Durand and L. Lee. "On-chip diagnostic equipment for 100 GHz superconducting circuits." IEEE Trans. Magn., vol. 27, pp. 3370-3373, Mar. 1991.

[4] A. Larsen. H. D. Jensen, and J. Mygind. "Josephson tunnel junction coupled to superconducting thin film resonator." Physica B, vol. 165, pp. 103-104, 1990.

[5] A. H. Dayem and C. C. Grimes. "Microwave emission from superconducting point-contracts." Appl. Phys. Lett., vol 9, pp. 47-49, July 1966.

[6] O. H. Soerensen. N. F. Pedersen. J. Mygind. B. Dueholm. T. F. Finnegan. J. B. Hansen, and P. E. Lindelof. "Microstrip coupling techniques applied to thin film Josephson junctions at microwave frequencies," IEEE Trans. Magn., vol. MAG-17, pp. 107-110, Jan. 1981.

[7] A. K. Jain. K. K. Likharev. J. E. Lukens, and J. E. Sauvageau. "Mutual phase locking in Josephson junction arrays." Phys. Rep., vol. 109, p. 309, 1984.

[8] K. Wan. B. Bi. A. K. Jain. L. A. Fetter. S. Han. W. H. Mallison, and J. E. Lukens. "Refractory submillimeter Josephson effect sources." IEEE Trans. Magn., vol. 27, pp. 3339-3342, Mar. 1991.

[9] J. E. Sauvageau. "Phase-locking in distributed arrays of Josephson junctions." Ph.D. dissertation. SUNY at Stony Brook. unpublished.

[10] W. H. Chang. "The inductance of a superconducting strip transmission line." J. Appl. Phys., vol. 50, no. 12, pp. 8129-8134, Dec. 1979.

[11] K. C. Gupta. R. Garg. and I. J. Bahl. Microstrip Lines and Slotlines. Dedham, MA: Artech House, 1979.

[12] R. L. Kautz. "Picosecond pulses on superconducting striplines." J. Appl. Phys., vol. 49, no. 1, pp. 308-314, Jan. 1978.

[13] D. C. Mattis and J. Bardeen. "Theory of the anomalous skin effect in normal and superconducting metal." Phys. Rev., vol. 111, pp. 412-418, 1958.

[14] W. H. Henkels and J. C. Kircher. "Penetration depth measurements on type II superconducting films." IEEE Trans. Magn., vol. MAG-13, pp. 63-66, Jan. 1977.

[15] H. K. Olsson. "Dielectric constant of evaporated SiO at frequencies between 13 and 103 GHz." IEEE Trans. Magn., vol 25, pp. 1115-1118, Mar. 1989.

[16] L. Lewin. "Spurious radiation from microstrip." Proc. Inst. Elec. Eng., vol. 125, pp. 633-642, July 1978.

[17] R. Pöpel. "Measured temperature-dependence of attenuation constant and phase velocity of a superconducting PbAu SiO Pb microstripline at 10 GHz and 30 GHz." IEEE Trans. Microwave Theory Techn., vol. MTT-31, pp. 600-604, 1983.

Baokang Bi received the B.S. Degree in physics from the University of Science and Technology of China (USTC) in 1982 and the M.S. degree in physics from the Cryogenic Lab. Chinese Academy of Science in 1986. Since 1987 he has been a graduate student in the Department of Physics. State University of New York at Stony Brook.

His current research interests include the low and high T_c superconducting electronics and applications especially the design. fabrication and test of submillimeter wave devices.

K. Wan. photograph and biography not available at time of publication.

Wenxing Zhang received the B.S. degree in electrical engineering from the Department of Physics. NanKai University, China in 1982, and the M.S. degree in applied physics from the Beijing University of Aeronautics and Astronautics in 1986.

From 1986 to 1989. he was a Physics Lecturer with the Beijing University of Aeronautics and Astronautics and did research on the magnetic properties of amorphous materials. Since 1990, he has been a Visiting Scientist in the Department of Physics. State University of New York at Stony Brook. His research interests include superconductive microwave circuit design, fabrication, and test.

Siyuan Han received the B.S. degree from the University of Science and Technology of China in 1982 and the Ph.D. in physics from Iowa State University, Ames, in 1986.

He is presently a Research Assistant Professor at the State University of New York at Stony Brook where he is involved in research projects studying fundamentals and device applications of the Josephson effect.

James E. Lukens received the B.S. degree from Stanford University in 1963 and the Ph.D. from the University of California, San Diego, in 1969.

He is presently a Professor of Physics at the State University of New York at Stony Brook where he is Project Director for a number of research projects studying fundamentals and device applications of the Josephson effect.

DISTRIBUTED JOSEPHSON JUNCTION ARRAYS AS LOCAL OSCILLATORS

Baokang Bi, S. Han, J. E. Lukens, and K. Wan*

Department of Physics
SUNY at Stony Brook, Stony Brook, NY 11794

Abstract - The power and linewidth of the radiation, near 250 GHz, of small distributed Josephson junction array sources have been measured using a single chip integrated source and receiver. The one-dimensional arrays were of a new design with junctions placed in 1/4 wavelength lumps separated by one half wavelength. The measured power ($\simeq 2\,\mu W$) and linewidth ($\simeq 10$ MHz) for the 10 junction sources were in reasonable agreement with those obtained from computer simulations.

I. INTRODUCTION

Over the last decade, Josephson junction arrays have been demonstrated to be useful for generating radiation in the millimeter and submillimeter wave ranges[1-4]. The first generation of Josephson junction arrays were lumped circuits, requiring that the distribution of junctions should be within one-eighth of a wave length at the operating frequency. Such a requirement limits the maximum number of junctions that can be accommodated, and therefore the maximum available power level. The "quasi-lumped"[4] array, in which junctions were placed one wave length apart, was developed to remove this limitation. Experimental results on quasi-lumped arrays have demonstrated their ability to deliver higher output power to a high impedance load. However, the design of the quasi-lumped array results in a large structure, which is less compact and, more importantly, has significant transmission line loss at high frequency.

In this paper, we report an improved design for one dimensional Josephson junction arrays, incorporating the concepts of both lumped and quasi-lumped arrays. In this new design, junctions are separated into groups with an inter-group spacing of half a wave length, see Fig. 1. This structure approximates that of the quasi-lumped array. However a group of junctions, which, in principle, can be distributed over a length up to $1/2\,\lambda$, replaces each single junction used in the previous design. This new array is distributed in nature. The improved design not only reduces the internal loss, but also increases the available power density since the total length of the array is reduced dramatically. The performance of these

distributed arrays is studied here both by computer simulation and measurement on actual devices.

II. SIMULATION

To optimize the design of the distributed array, we need to determine the junction position along the microstrip so that all the junctions are strongly phase locked with a nearly constant phase with respect to the RF current in the microstrip. A computer simulation has been carried out to study the behavior of such an array. The simulation is based on the perturbation theory[5] of the Resistively Shunted Junction (RSJ). For a N junction one dimensional array, if the junctions are dc biased in series, then the voltage across the mth junction can be expressed as[5,6]

$$\dot{\theta}_m = \omega^u_m + \alpha_m \frac{2\pi}{\Phi_0} R_{dm} I_{rf} \qquad (1)$$

where I_{rf} is the total RF current going through the mth junction due to all the junctions in the arrays

$$I_{rf} = \prod_{k=1}^{N} \epsilon_k \mid Y_{mk}(\omega) \mid \cos(\gamma_{mk} + \theta_m - \theta_k) \qquad (2)$$

and ω^u_m, α_m and R_{dm} are the voltage, the down conversion coefficient and the dynamical resistance of the mth junction respectively in the absence of interactions. ϵ_k is the rf voltage amplitude generated by the kth junction. The interactions among junctions are included in the equation through the complex mutual admittance Y_{mk} with phase γ_{mk}. The linear component of the phase of each junction is given by θ_m. For given operating voltage $v = V/I_c R_J$, junction parameters ω^u_m, α and ϵ, can be calculated[5].

For an N junction array, Eqs. 1 and 2 give a set of $2N$ coupled equations. To study the phase locking behavior, these $2N$ equations must be solved simultaneously. Phase locking is achieved once the voltages $\dot{\theta}_m$ across all the junctions become equal. This locking process can be quite complex in the type of resonant structure studied here since Y_{mk} can vary rapidly with frequency near the operating point. The structure, as shown in Fig. 1a, is typical of those studied. The total length of the array is 400 μm long, about one wave length at an operating frequency $f = 300$ GHz. The 20 junctions in the array are separated into two groups. The inter-junction spacing within each group is 10 μm, and the inter-group spacing is 200 μm, or a half wave length at the designed frequency. The array is

terminated at the right end with a load $Z_l = 30\,\Omega$. In the computer simulation, identical RSJs are assumed with normal resistance $R_j = 0.5\,\Omega$, and $I_c R_j = 600\,\mu V$. The simulation process starts with randomly given initial phases for all the junctions. The iteration proceeds until the phase locking condition is achieved. The simulation results reveal several important features of distributed arrays.

A. Distributions of rf current and junction phase

The distributions of RF current and the phase difference $\Delta\theta \equiv \theta_{junction} - \theta_{rf}$ between the junction and RF current at $320\,\text{GHz}$ ($l=1.18\,\lambda$) are shown in Fig. 1b when all the junctions are phase locked. The horizontal axis in Fig. 1b represents the locations of junctions in the array. As expected, a strong resonance is established. The magnitude of the rf current follows the profile of a standing wave. It can be noted that there is an
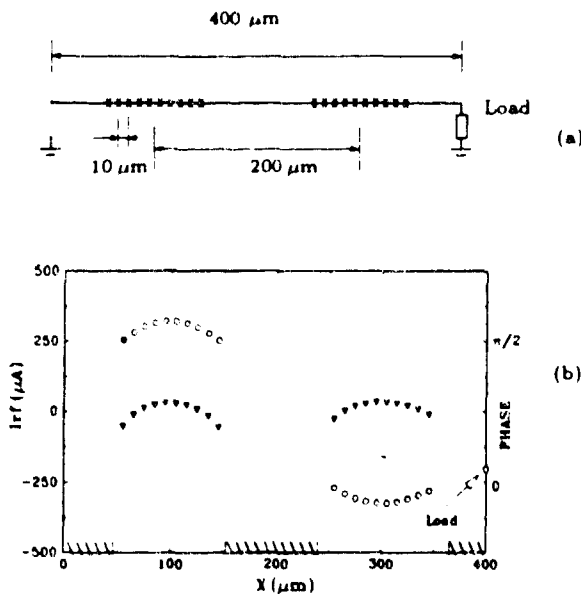

Fig. 1 (a) The structure of the array. (b) Amplitude of RF current (O) and the phase difference $\Delta\theta$ (∇).

appreciable RF current ($I_{rf} = 203\,\mu A$) going through the load, i.e. a traveling wave component is also present near the load.

B. Stability of phase locking

The stability of phase locking is usually measured by the range in bias current over which phase locking can be sustained[5]. It has been shown that this stability of phase locking is related to the phase difference $\Delta\theta$ between the junction and the RF current[5]. Once phase locked, the phase difference is always within 0 and π with the maximum stability at $\pi/2$ and the least

stability at 0 and π. By applying this stability rule, one can observe from Fig. 1b that the junctions located near the RF current anti-nodes are the most stable. The shaded areas indicate the unstable regions where no junctions should be placed. The existence of these less stable regions is due to the low RF current amplitude and the less ideal phase differences both of which reduce the locking strength.

III. INTEGRATED SUBMILLIMETER WAVE RECEIVER

The above simulation results outline the basic design rules for the distributed array. Arrays with the same parameters as those shown in Fig. 1a have been fabricated. To evaluate their performance, we performed both RF power and radiation linewidth measurements. In order to measure the radiation linewidth in the submillimeter wave range, we designed a prototype Integrated Submillimeter Wave Receiver (ISWR) schematically shown in Fig. 2. Here two arrays, a Josephson effect detector and an SIS mixer are integrated on a single silicon substrate. One array functions as the local oscillator and pumps the SIS junction. The other array, weakly coupled, serves as the signal source. Both arrays have the same design parameters. The load for these arrays is the SIS mixer with a normal state resistance R_n between 20 to 40 Ω. As shown in
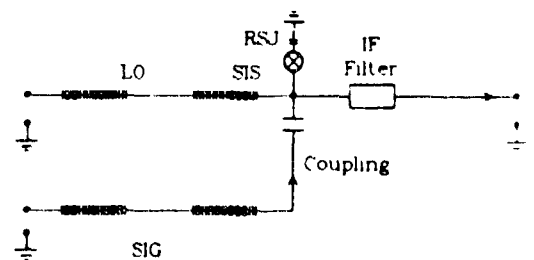

Fig. 2 Schematic of Integrated Submillimeter Wave Receiver.

Fig. 2, the SIS mixer is grounded via a lower impedance ($\sim 0.5\,\Omega$) RSJ junction. The primary function of this single RSJ is to measure the rf current, therefore the rf power, delivered to the SIS junction from the local oscillator array. Also included on the chip are an IF filter, a coupler/dc block and a dc bias network. The characteristic impedance of the microstrip transmission line is 20 Ω. The IF signal, coming from microstrip, passes through the on-chip IF filter and goes to a 50 Ω SMA connector via a 50 Ω coplanar wave guide transition. These impedances are chosen so that there is a reasonable impedance match between different sections. However, no effort has been made to optimize them.

In order that the two arrays can be frequency tuned independently, phase locking should not exist between them. One function of the small coupling capacitor in the microstrip is to isolate the two arrays so that the measured locking range corresponds to only about 10% of their frequency difference at the 10 GHz IF frequency. The required LO power, based on the optimum pumping power equation from Tucker's theory[7], is

$$P_{LO} = (\hbar\omega a/e)^2/2R_n \qquad (3)$$

where ω is the LO pumping frequency and R_n is the normal state resistance of the SIS junction. The dimensionless variable $a = eV_{LO}/\hbar\omega$, is a measure of the LO power level. Assuming all the junctions are in phase, one can estimate the power delivered to the SIS mixer as

$$P = \frac{1}{2}(\frac{N\epsilon}{NR_j+R_n})^2 R_n \qquad (4)$$

where ϵ is the RF voltage generated by each junction. This implies that a minimum of 6 junctions are needed for the 110 nW required pumping power, assuming $R_j = 0.5\,\Omega$, $R_n = 25\,\Omega$ and $a \simeq 2$. The value of a is chosen based on the assumption that, the conversion is on the peak of the first Bessel function $J_1(a)$[7].

The fabricated ISWR is designed to operate around 300 GHz. The RSJ junction area is $2 \times 2\,\mu m^2$, which requires a current density $J_c = 30\,kA/cm^2$ for the desired $I_c = 1\,mA$. Low inductance ($L \simeq 0.1\,pH$) Au resistors are used for resistive shunts. For the SIS mixer, the ωRC product is designed close to 3. With $R_n \simeq 20$ to 30 Ω, a $J_c = 4\,kA/cm^2$ is necessary for the $1 \times 1\,\mu m^2$ junction used. Because these current densities are quite different, two separate Nb/AlO/Nb tri-layers with different oxidation times were used. The detailed Nb junction fabrication process can be found in reference 4. In the design, contrary to the simulation, the junctions in the array are parallel biased in order to compensate for the non-uniformity of junction parameters. Each 10 junction section of the array can be biased independently.

IV. EXPERIMENTS AND RESULTS

All the experiments were done in a μ-metal and lead can shielded dewar with the sample immersed directly in liquid helium. All the junctions/arrays were powered by batteries with careful filtering. The output power from the 20 junction LO array was measured, using the SIS junction biased at 8 mV, where it has a resistance of 26 Ω, as the load. The Shapiro step width of the single RSJ detector junction in series with the SIS junction was used to determine the RF current through this load. Figure 3 shows the RF power measured at 1.57 K as a function of LO frequency. The maximum power of 1.8 μW is obtained at the designed resonant frequency of

300 GHz. The dash line is the expected power calculated by assuming the in-phase operation of all the junctions. Eq. 4. The effect of junction's shunt inductance on the RF power measurement is estimated to be less than 13% at 300 GHz. The data show that the LO array delivered full power to the load, implying that all the junctions in the distributed array oscillate coherently and in phase.

The radiation linewidth is measured by using a double heterodyne mixing technique. The first mixing is done on chip using the ISWR. The first IF output, typically 10 to 18 GHz, is then brought out of the He dewar via semi-rigid coaxial cable. It is mixed with a second microwave LO giving the second IF at 100 MHz, which is coupled to the detector through an IF bandpass filter whose bandwidth varies from 1 MHz to 4 MHz. The I-V curves of the SIS mixer junction are shown in Fig. 4. Curve a is the unpumped SIS junction. The lack of
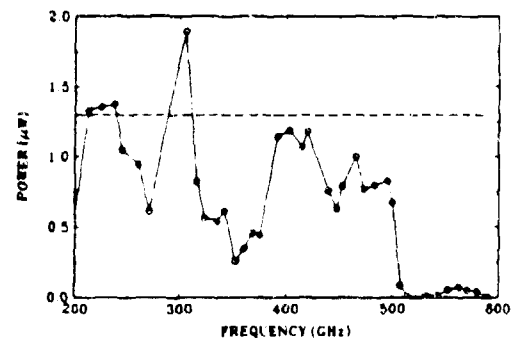

Fig. 3 Measured RF power spectrum (o) from 20 junction LO array delivered to SIS junction biased at 8 mV (R_n=26 Ω) at 1.57 K. Dashed line is the estimated power from Equ. 4.
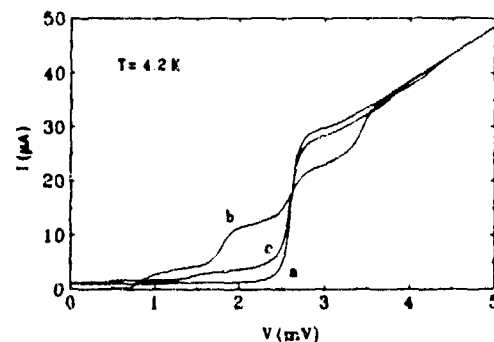

Fig. 4 I-V curves of SIS with 10 junction LO array off (a) and on (b, c).

apparent supercurrent in these curves is probably due to the trapped magnetic flux. Traces b and c are the pumped I-V curves when the local oscillator array was operating at 210 GHz and 312 GHz respectively. The

quasi-particle steps can be clearly seen both below and above the gap voltage. When the ISWR is operating in the receiver mode for the linewidth measurement, the 20 junction LO array delivers too much power to the SIS mixer. To cut down the pumping power, only 10 junctions are used. It seems that the power coupled to the SIS mixer at 210 GHz is still higher than the optimum level.

During linewidth measurements, the signal array is biased at 256 GHz whereas the LO array is biased at 240 GHz. The SIS mixer is biased at the center of the first quasi-particle step where the maximum response is expected. The spectrum of the first IF taken at 1.57 K is
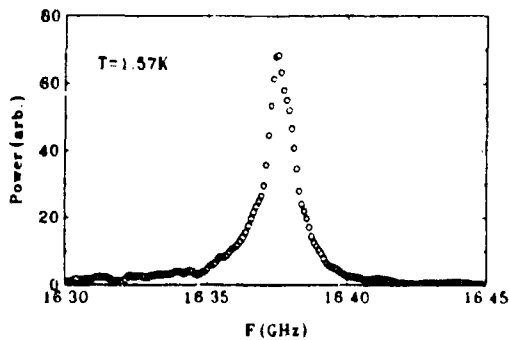

Fig. 5 Radiation spectrum taken at 1.57 K.

shown in Fig. 5. At this temperature, the measured linewidth $\Delta f = 10.3$ MHz, which is the convolution of the linewidths from LO and SIG arrays, is about 50% larger than the linewidth estimated by assuming that the noise is entirely due to the Nyquist noise of shunt resistors. At 4.0 K, the measured linewidth, 23.1 MHz, is 15% larger than that estimated. Both the low frequency and the down converted high frequency noises are included in the estimate. A more detailed linewidth analysis will be published elsewhere.

VII. CONCLUSION

A single chip receiver and signal source operating near 250 GHz, using Josephson effect array oscillators and an SIS mixer has been fabricated and tested. The IF, coupled off the chip to a room temperature spectrum analyzer, permitted a direct measurement of the oscillator linewidth. The arrays were of a new design, with junction distributed over a substantial part of a wavelength. The measured power and linewidth were in good agreement with those obtained from computer simulations, implying complete in phase locking of the sources.

ACKNOWLEDGEMENTS

REFERENCES

[1] A. K. Jain, P. Mankiewich, and J. E. Lukens, "Observation of Phase Coherence Among Multiple Josephson Oscillators," *Appl. Phys. Lett.*, 36, 774 (1980).

[2] J. E. Sauvageau, A. K. Jain, and J. E. Lukens, "Millimeter Wave Phase-locking in Distributed Josephson Arrays," *Int. J. Infrared and Mm Waves*, vol. 8, 1281(1987).

[3] S. P. Benz, and C. J. Burroughs, "Coherent Emission from Two-dimensional Josephson Junction Arrays," *Appl. Phys. Lett.*, 58, 2162(1991).

[4] K. Wan, B. Bi, A. K. Jain, L. A. Fetter, S. Han, W. H. Mallison, and J. E. Lukens, "Refractory Submilli meter Josephson Effect Sources," *IEEE Trans. Magn.*, MAG-27, 3339(1991).

[5] A. K. Jain, K. K. Likharev, J. E. Lukens, and J. E. Sauvageau, "Mutual Phase locking in Josephson Junction Arrays," *Phys. Rep.*, 109, 309(1984).

[6] J. E. Sauvageau, "Phase-locking in Distributed Arrays of Josephson Junctions," Ph. D. dissertation. SUNY at Stony Brook, (unpublished, 1987).

[7] J. R. Tucker and M. J. Feldman, "Quantum Detec tion at Millimeter Wavelengths," *Rev. Mod. Phys.*, vol. 57, 1055(1985).

Radiation linewidth of phase-locked distributed array in the submillimeter wave range

Baokang Bi, Siyuan Han, and James E. Lukens
Department of Physics, State University of New York at Stony Brook, Stony Brook, New York 11794

The radiation linewidth of a phase-locked distributed Josephson junction array source at 250 GHz has been measured as a function of temperature using an integrated submillimeter wave receiver/source. The measured total linewidth (including signal and local oscillator arrays, having 10 junctions each) is 10 MHz at 1.6 K. The measured data agree, within 50% uncertainty, with the linewidth obtained from computer simulation assuming the Nyquist noise current spectral density generated by the junction shunt resistors.

The development of sources based on the phase-locked arrays of Josephson junctions[1-3] has reached a state where a useful power level[3] (several μW) can be delivered to a high impedance load (20–60Ω) in the submillimeter wave range. However, measurements of the linewidth for these arrays have not been made. Previous measurements of the radiation linewidth of phase-locked Josephson junction arrays were performed between 2 and 20 GHz[1,4] on the lumped arrays, where the length, *l*, of the region containing junctions was much smaller than the wavelength, λ. The theoretically predicted dependencies of the radiation linewidth on the junction dynamic resistance and on the number of junctions were observed. The potentially much more useful array sources operating in or near the submillimeter wave range, however, have a distributed structure ($l > \lambda$). In this letter, we report and compare simulations and measurements of the radiation linewidth of phase-locked distributed Josephson junction arrays operating at 250 GHz.

The radiation linewidth of a single resistively shunted Josephson junction (RSJ) has been well studied,[1,5] and the predictions were verified experimentally.[6,7] For a RSJ, the noise is dominated by the Nyquist noise current generated by the shunt resistor R, producing a linewidth

$$\Delta\omega = \pi\left(\frac{2\pi}{\Phi_0}\right)^2 R_d^2 [S_I(0) + 2\alpha^2 S_I(\omega_0)],\qquad(1)$$

where R_d is the dynamic resistance of junction at the operating point, α is the down conversion coefficient, $\Phi_0 \equiv h/2e$ is the flux quantum, and $S_I(0)$ and $S_I(\omega_0)$ are the current noise spectral densities at low frequencies and at the Josephson frequency ω_0, respectively, and are given by the Nyquist formula including zero point fluctuations[7]

$$S_I(\omega) = \frac{\hbar\omega}{\pi R}\coth\left(\frac{\hbar\omega}{2k_B T}\right).\qquad(2)$$

For an array with N junctions, as shown in Fig. 1(a), there are N noise sources each of which contributes to the linewidth. Therefore the total linewidth for a phase-locked array, assuming these noise sources are incoherent, can be written as

$$\Delta\omega = \pi\left(\frac{2\pi}{\Phi_0}\right)^2 \sum_{m=1}^{N} R_{dm}^2 [S_{Im}(0) + 2\alpha_m^2 S_{Im}(\omega_0)]$$

$$= \pi\left(\frac{2\pi}{\Phi_0}\right)^2 [S_I(0) + 2\alpha^2 S_I(\omega_0)]\sum_{m=1}^{N} R_{dm}^2,\qquad(3)$$

where the last equal sign holds for identical junctions. Here $R_{dk} \equiv (\Phi_0/2\pi)(d\omega_0/dI_k)$ is the dynamic resistance of the kth junction and, in general, is affected by the interactions of the kth junction with other junctions in the array and with the circuit, e.g., by the rf current I_{rf} going through the kth junction. One of the great advantages of phase-locked arrays is that the oscillation linewidth is considerably narrowed compared to the linewidth of a single junction oscillator identical to those in the array. For a lumped array, the linewidth can be reduced by a factor of N since the junction's dynamic resistance R_{dk} can be $1/N$ of that of a single junction.[4] In a distributed array, however, this simple relation may not hold since I_{rf} can vary with position in the array, so R_{dk} must in general be determined by computer simulation.

We have numerically simulated the distribution of the junctions' dynamic resistances for the distributed array structures shown in Figs. 1(a) and 1(b). In these arrays, 20 junctions, in two groups of 10, are coupled together through a 20 Ω microstrip, which is designed to be one wavelength λ long at the intended operating frequency of 300 GHz. As seen in Fig. 1(b), the left end of the transmission line is open, and the other end is either terminated with a load (upper array), which, in this case, is a superconductor-insulator-superconductor (SIS) mixer junction with a normal state resistance of about 30 Ω, or is weakly coupled to the mixer (lower array) through a capacitor. The interjunction spacing is 10 μm, and the center to center intergroup spacing is 200 μm, i.e., $\lambda/2$. The RSJs used in the arrays have resistive shunts with a designed $I_c R \approx 600$ μV and $R = 0.9$ Ω. With these parameters, the normalized voltage, $V/I_c R$, is close to unity at the designed operating frequency. This assures that the radiation from the RSJ is almost monochromatic, and at the same time the phase locking among junctions is the strongest.

The computer simulation used to determine R_{dk} is based on a perturbation theory[1] where the phase-locking rf current through a junction in the microstrip is treated as a perturbation to the analytical solution of the RSJ model,
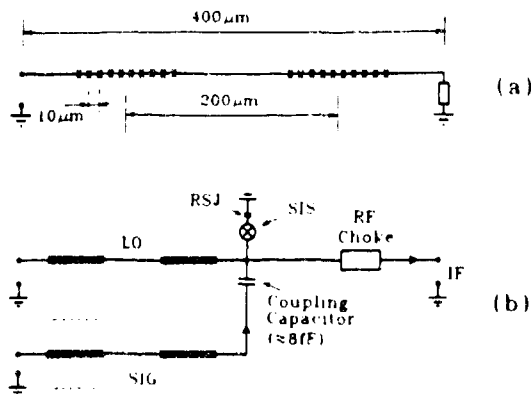
18

FIG. 1 (a) Structure of distributed Josephson junction array designed to have a resonance at 300 GHz. The right end is terminated with a load of 30 Ω. (b) Layout of integrated submillimeter wave receiver/source. The signal array (bottom) is weakly coupled to the SIS mixer. The IF is coupled off the chip and measured by a room-temperature spectrum analyzer. For clarity, only the dc bias of one section of the parallel biased SIG array is shown (dashed line).

FIG. 2. Calculated junction dynamic resistance as a function of junction position in the LO array when 20 junctions were used (solid squares), and in the LO array (down solid triangles), and in the SIG array (up solid triangles) with only the 10 junctions nearer the mixer operating. The rf current (open circles), when 20 junctions are used, is also shown

which is denoted through superscript u. e.g., $\omega^u(I)$. The rf current I_{rf} is related to the junctions' oscillations through the frequency dependent admittances[8] $Y_{km}(\omega)e^{\gamma_{km}}$. The N phase-locking equations for the frequencies of the junction oscillation can be written as

$$\omega_k(I_k) = \omega_k^u(I_k) + \left(\frac{2\pi}{\Phi_0}\right) \sum_{m=1}^{N} \alpha_k \epsilon_m R_{dk}^u Y_{km}(\omega)$$

$$\times \cos(\gamma_{km} + \theta_m - \theta_k), \qquad (4)$$

where ϵ_k is the magnitude of the fundamental Josephson oscillation, and θ_k is the linear component of the kth junction's phase. In order to calculate the dynamic resistance R_{dk} of individual junctions in the phase-locked array, the dc voltage change was determined as the bias current through the kth junction was varied while holding all other biases constant. In Fig. 2, the dynamic resistances R_{dk} (solid squares), together with the rf current I_{rf} (open circles), are plotted as a function of junction position in the array operating at a frequency such that the wavelength $\lambda = 0.8l$. As can be seen, the dynamic resistance varies from junction to junction, reflecting the distributed nature of this array. The average of $R_{dk} = 37$ mΩ is slightly less than that of $R_{dk}^u/N = 54$ mΩ expected from a lumped array due to the resonant structure of the array. Also shown in Fig. 2 are the calculated R_{dk} for both the upper (down solid triangles) and the lower arrays (up solid triangles) when only the group of 10 junctions nearer the mixer are biased.

To measure the radiation linewidth in the submillimeter wave range, we have developed an integrated submillimeter wave receiver/source (ISWR/S).[3] This contains two arrays, having the same dimensions as shown in Fig. 1(a), and one SIS mixer junction, fabricated using Nb/AlO$_x$/Nb technology. The upper array serves as the local oscillator (LO) and pumps the SIS mixer, the other (weakly coupled) serves as the signal source (SIG). All of the junctions were powered by low noise battery operated power
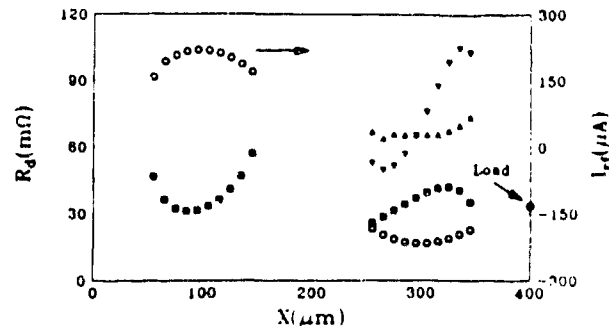
supplies, which gave a negligible contribution to the linewidth. While the different groups of junctions could be biased independently, junctions within a group were biased in parallel from a common source through a series of interlocking dc superconducting quantum interference device loops[1,3] having a high impedance at ω_0. All voltage leads were filtered by an 8-ms RC filter, whereas the high current bias leads were filtered by 14-ms RC filter.

The power spectral density of the radiation was measured by using a double heterodyne mixing technique. The signal from the SIG array, operating at 255 GHz, was mixed down to an $IF = 15$ GHz by the on chip SIS mixer, which was pumped by the LO array oscillating at 240 GHz. One reason for selecting this relatively high IF frequency was to ensure that the interaction of the two weakly coupled arrays did not affect their linewidth. To obtain the proper power level from the LO array, only the groups of 10 junctions closer to the SIS mixer were actually used. The IF was coupled via coaxial cable out of the cryostat where it was further mixed down to 110 MHz and detected. An isolator, inserted at the top of the cryostat, prevented signals and noise from the room-temperature electronics from coupling back to the sample. The bandwidth of the second IF bandpass filter, 1 MHz for $T < 2.5$ K, and 4 MHz for $T > 2.5$ K, determined the frequency resolution in the spectrum measurements. The detected power has, in the worst case, a peak signal to background noise ratio larger than 5. This background noise was subtracted from the measured spectrum. The solid circles in Fig. 3 show the measured total linewidth (LO array plus SIG array) as a function of liquid helium bath temperature from 4.0 to 1.5 K.

In order to accurately calculate the expected linewidth, one needs to know the dynamic resistance of each junction as well as the current noise spectrum. Our parallel bias scheme made it impossible to directly measure the dynamic resistance of individual junctions. However, the dynamic resistances of the arrays could be measured and used to estimate the junctions' dynamic resistances based on the simulation. The dynamic resistance of the LO (SIG) array varies from 65 mΩ (58 mΩ) at 4.2 K, to 55 mΩ (40 mΩ)
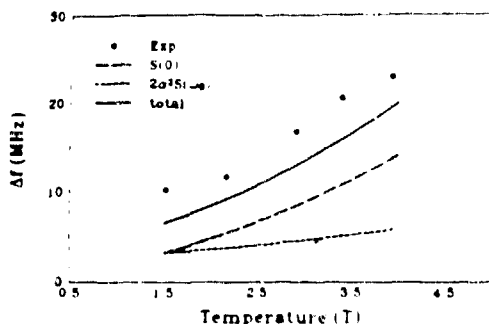
19

FIG 3 Measured radiation linewidth (solid circles) as a function of temperature The solid line is the calculated total linewidth The long dashed line is the contribution from low frequency current noise The short dashed line is the contribution from high frequency current noise including zero point fluctuations at Josephson oscillation frequency

at 1.57 K. The linewidths of the individual arrays are then calculated from Eq. (3) using the calculated values of R_{dk}, shown in Fig. 2(b), scaled to give an average equal to the measured parallel dynamic resistance. This introduces an estimated uncertainty of about 30% for the calculated linewidth. An additional uncertainty in the comparison of the calculated and measured linewidth is introduced by the convolution of the LO and SIG linewidths during the on chip mixing. The finite linewidth of the LO array affects the total linewidth through the change of mixer gain, which is mainly a function of the LO power, within the linewidth of the LO array. Around the usual applied LO pumping power level (< the optimum LO pumping power),[9] the mixer conversion gain is roughly proportional to the applied LO power.[10] Such a relation gives a convoluted linewidth equal to the sum of the two linewidths, assuming Lorentzian line shapes. The nonlinear gain-power relation of the physical mixer could introduce an error of about 10% in the convoluted linewidth. The solid

line in Fig. 3 shows total linewidth calculated from Eqs. (2) and (3) using these approximations.

Our measured linewidths from 10 junction distributed arrays sources agree with those expected from the Nyquist noise due to the junctions' shunts within the 50% uncertainty of our comparison. This indicates that additional noise sources such as the shot noise of tunnel currents or coherent rf noise currents coupled via the coaxial cable are not dominate. The analysis presented can therefore serve as a guide to the expected linewidths in the much larger arrays being developed as practical submillimeter sources where, for constant array impedance, one expects $\Delta \omega \propto 1/N^2$.

A K Jain, K K Likharev, J E Lukens, and J E Sauvageau, Phys Rep 109, 309 (1984)

A Davidson, IEEE Trans Magn MAG-17, 103 (1981), J E Sauvageau, A K Jain, and J E Lukens, Int J Inf MMW 8, 1281 (1987), M J Lewis, D Durand, A D Smith, and P Hadley (unpublished), S P Benz and C J Burroughs, Appl Phys Lett 58, 2162 (1991)

B Bi, S Han, J E Lukens, and K Wan, IEEE Trans Appl Superconductivity (to be published), K Wan, B Bi, A K Jain, L A Fetter, S Han, W H Mallison, and J E Lukens, IEEE Trans Magn MAG-27, 3329 (1991)

A K Jain, P M Mankiewich, A M Kadin, R H Ono, and J E Lukens, IEEE Trans Magn MAG-17, 99 (1981)

R H Koch, D J Van Harlingen, and J Clarke, Phys Rev Lett 45, 2132 (1980)

A H Silver, J E Zimmerman, and R A Kamper, Appl Phys Lett 11, 209 (1967)

R H Koch, D J Van Harlingen, and J Clarke, Phys Rev Lett 47, 1216 (1981)

J E Sauvageau, Ph D thesis, SUNY at Stony Brook, 1987

J R Tucker and M J Feldman, Rev Mod Phys 57, 1055 (1985)

C A Mears, Q Hu, P L Richard, A H Worsham, D E Prober, and A V Raisanen, Appl Phys Lett 57, 2487 (1990)

20

COMPLETE PHASE-LOCKING IN A ONE-DIMENSIONAL SERIES BIASED JOSEPHSON-JUNCTION ARRAY

Siyuan Han, A. H. Worsham, and J. E. Lukens

Department of Physics

SUNY at Stony Brook

Stony Brook, NY 11794

Abstract — The rf power at ~ 300 GHz coupled to a 52 Ω load by a one-dimensional dc series biased Josephson junction array has been measured using an on-chip Josephson detector. From the measured rf power and dc voltage levels we conclude that the 100 junctions in this 1D array were locked in-phase. The effects of the finite inductance, associated with the junction's shunt resistor, on array's output power and detector's current-voltage characteristics are also discussed.

I. INTRODUCTION

Phase locked Josephson junction arrays have many advantages over single junction oscillators as millimeter and submillimeter sources. Compared to a single junction of shunt resistance R_s and characteristic voltage $V_c \equiv I_c R_s$ where I_c is critical current, a one-dimensional (1D) rf series array of total resistance R_s consisting of N junctions, each having the same characteristic voltage V_c as that of the single junction, is expected to increase the rf power delivered to a matched load $R_L = R_s$ by N^2 times, and to reduce the radiation linewidth by a factor of N^2 while preserving the rapid tuning speed of the single junction source [1-3]. All of these properties of the 1D array have been experimentally demonstrated recently [4-7] in arrays having several tens of junctions. For example, the rf power delivered to a 60 Ω load at 350 GHz was observed to be equal to the maximum expected power of a completely phase locked array [4]. (Recently published results of computer simulations of 1D arrays [8] showing a maximum power far less than the coherent sum of the powers from the individual junctions are not applicable to our work, since these simulations did not include any phase-locking interactions among the junctions.)

II. EXPERIMENT

For the experimental results referred to above, the scatter in the junction parameters within the arrays made it necessary to use a parallel dc bias scheme to achieve phase locking in these rf series arrays [4,5]. Our simulations show that, for example, a scatter in I_c of less than $\pm 7\%$ is required to achieve phase locking with series dc biasing. Series biasing is never-the-less desirable
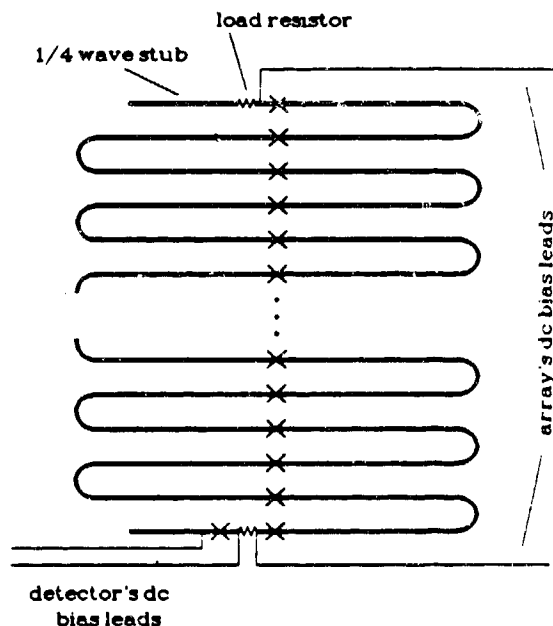
Fig. 1. Schematic of the 100-junction series biased 1D array (x represents the Josephson junction).

since it requires much lower bias currents [9] and permits the use of various shunting schemes for line-width reduction. Here, we report new results on a 1D array of *series dc biased* junctions which was fabricated at IBM by the Consortium for Superconducting Electronics (CSE) using the Planarized All-Refractory Technology for low-T_c Superconductivity (PARTS) developed by Ketchen *et. al* [10]. This new technology produced a 100-junction 1D array with a spread in I_c of about $\pm 3\%$.

This 100-junction 1D array was designed to test both the long standing predictions for phase-locking with series bias and whether the current fabrication technology for Nb based Josephson junctions could provide adequate junction uniformity for complete phase locking. As seen in the schematic of the array in Fig. 1, the junctions are placed at intervals of $\lambda_0 = 370$ μm along a 20 Ω serpentine microstrip transmission line. Both ends of the transmission line are terminated by quarter wave ($\lambda_0/4$) stubs. The detector junction has

the same nominal critical current and shunt resistance as the junctions in the array. For such an array of ideal resistively shunted junctions operated at frequency $f \approx v_p/\lambda_0$, where v_p is the phase velocity of the transmission line, the maximum power delivered to a resistive load R_L is

$$P_N = \frac{(NV_c)^2 R_L}{2(R_s + R_L)^2} \qquad (1)$$

where $R_s = NR_J$ if all the junctions are identical. Eq. 1 is exact only for average dc bias voltages of each junction $V \equiv V_{array}/N \gg V_c$.

The power delivered to the load R_L is measured by the amplitude of the constant voltage step in the detector's dc current-voltage characteristics (IVC). The critical current is measured from the IVCs of the array to be 80 μA at $\sim$ 1.4 K. The total resistance of the array $R_s = 162$ Ω is measured from the IVC with the Josephson current completely suppressed by applying a magnetic field, giving the mean shunt resistance per junction $R_J = 1.62$ Ω. The damping parameter $\beta_c \equiv 2\pi V_c R_J C/\Phi_0$ of the junctions is estimated to be $\sim$ 0.07, where C is the junction capacitance and $\Phi_0 \equiv h/2e$ is the flux quantum. The IVC/junction of the 100 junctions in series and the IVC of the detector are shown in Fig. 2. These IVCs are nearly identical showing the very good uniformity in I_c and R_J among all the junctions ($\sim$ 3%). In Fig. 3 the detector's IVC, for the array biased at 62.4 mV, is shown to clearly

from the size of the current step (n=1 Shapiro step) is $I_{rf} = 93$ μA. The value of $R_L = 52$ Ω, as determined from the IVC of the load resistor, thus gives the rf power delivered to the load resistor as 0.22 μW.
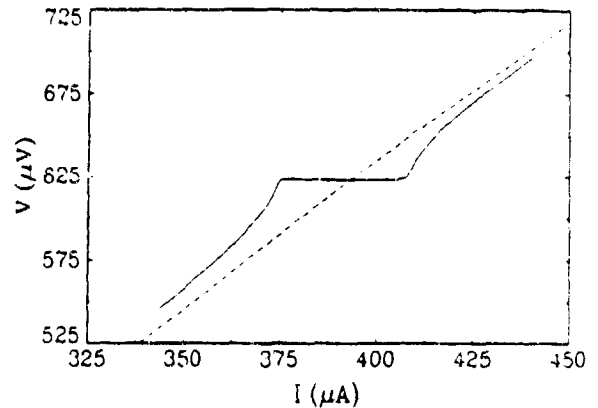
Fig. 3. Detector junction's IVC with array biased at V_{array}=62.4 mV (solid line) and array off (dashed line).

The value of $I_{rf} = 93$ μA is derived using a modified Resistively Shunted Junction (RSJ) model — Resistively-Inductively and Capacitively Shunted Junction (RICSJ) model — for the detector junction which takes into

(a)

(b)
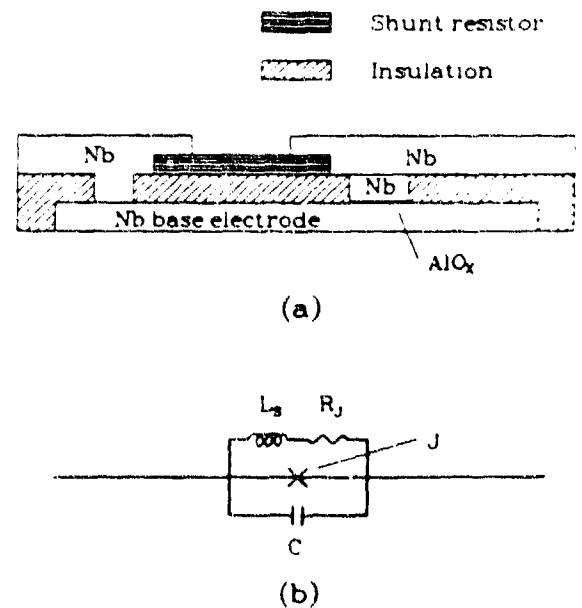
Fig. 4 (a) Schematics of a Resistively-Inductively Capacitively Shunted Junction (RICSJ) and (b) its equivalent circuit.
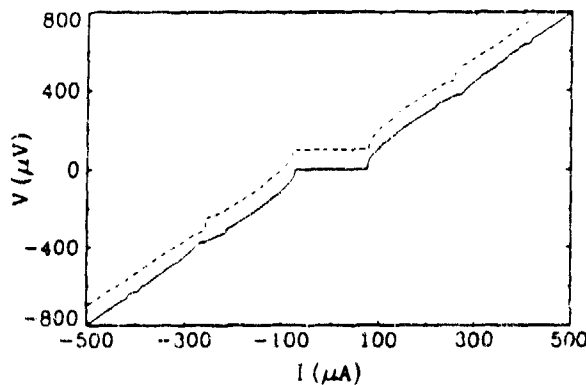

Fig. 2. IVCs of the array and the detector. The array's voltage is shown as the total voltage divided by the number of junctions (N=100). For clarity, the detector's IVC (dashed line) is shifted vertically.

display a current step at 624 ± 0.2 μV, i.e. at V_{array}/100. The amplitude of the rf current derived

account the finite inductance associated with the external shunt resistor placed across the tunnel junction. According to RSJ model the size of the first Shapiro step (~ 34 μA) requires the detector junction be irradiated an rf current having 200 μA amplitude, giving the rf power coupled to the load resistor to be about 1 μW. However, the existence of the parasitic inductance associated with the shunt resistor (cf Fig. 4) substantially increases the fraction of the external rf current flowing through the tunnel junction when the frequency $f \geq (R_s/L_s)/2\pi$. This, in turn, increases the step amplitude for a given rf amplitude (in the linear response range). Fig. 5 shows the relationship between
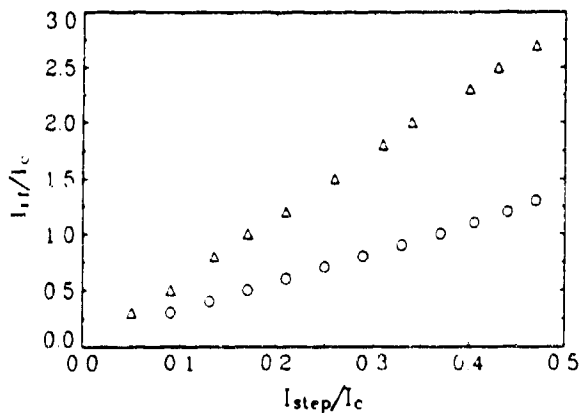

Fig. 5 Size of n=1 Shapiro step I_{step} vs. applied rf current amplitude I_{rf} of the RSJ model (open triangles) with $f\Phi_0 = 4.8\ V_c$, $\beta_c = 0.07$ and the RICSJ model (open circles) for $\beta_L = 0.22$ with same f and β_c, where $\beta_L \equiv 2\pi L_s I_c/\Phi_0$.

I_{rf} and I_{step} for the two different junction models based on our numerical simulations. A more detailed analysis of the RICSJ model will be published elsewhere.

III. DISCUSSION

This measured rf power coupled to the load is more than twice the value of $P_N = 95$ nW calculated from Eq. 1, using independently measured RSJ parameters. However, Eq. 1 is derived under the assumption that the junctions shunt inductance L_s is zero. In our sample, each junction has an inductance $L_s \sim 0.9$ pH in series with the shunt resistor (cf Fig. 4). Taking into account this inductance, the rf power coupled to the load would be increased to

$$P_L \simeq P_N \left\{ \frac{1+\alpha^2}{1 + [\alpha/(1 + R_L/R_s)]^2} \right\} \quad (2)$$

where $\alpha \equiv 2\pi f L_s/R_J$. This increase in the rf power coupled to the load is not hard to understand since the inductor provides considerable impedance at high frequencies $(2\pi f > R_s/L_s)$ hence reducing the rf power dissipated by the junction's shunt resistor. In deriving Eq. 2 we have made the assumption that tunnel junction's quasi-particle conductance $G_{qp} \ll 1/R_J$. For the tunnel junctions in the 1D array this is justified. According to Eq. 2 the rf power coupled to R_L at ~ 300 GHz should increase to 0.12 μW, still much lower than the observed value.

One of the possible explanations is that when rf current is close to or greater than the critical current of the junctions and the structure is resonant type, the perturbation approach and the lumped circuit approximation, which leads to Eqs. 1 and 2, is not adequate. It has been experimentally observed and confirmed by the numerical simulation that in a 1D array the rf current through the array can be several times I_c due to the strong coupling between series junctions embedded in a microstrip line and the resonator structure of the 1D array [1]. This explanation is supported by the resonant structure observed in the 1D array's IVC (cf. Fig. 6).
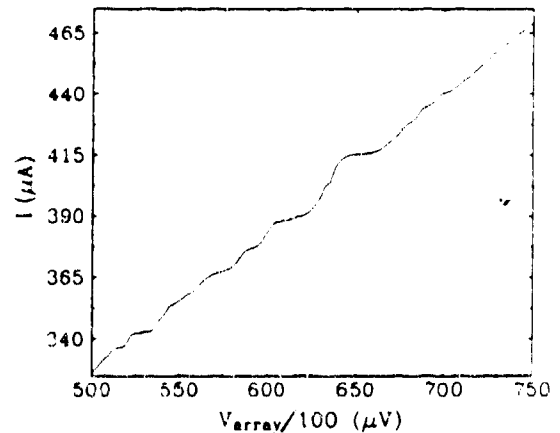

Fig. 6 Part of the IVC of the array showing the resonant structures.

While the maximum measured rf power is about twice that predicted (in the approximation used) we have a high degree of confidence in this result. In principle, independent of the junction and array model, the total power dissipated by all the junctions and the load at dc and the rf frequency should not exceed the input power supplied by the dc current bias source. As a check, we carefully measured the input power and the dc power dissipation and always find sufficient excess power to supply the rf power to the load.

IV. SUMMARY

In summary, we have demonstrated that complete phase locking has been achieved in a *series biased* 1D array fabricated using PARTS technology. While the design was restricted to rather low rf power due to the relatively low critical current density (~ 3 kA/cm^2) which was required for the rest of the devices (e.g. dc SQUIDs) on the same wafer, the measured rf power coupled to the 52 Ω load is 0.22 μW, exceeding the maximum power expected from the array by perturbation analysis. This observed rf power delivered to the load, along with the excellent agreement between the bias voltage of the array and the frequency of the detected radiation, provide strong evidence for complete in-phase locking of the junctions in this 100 junctions 1D array with series dc bias.

ACKNOWLEDGEMENT

REFERENCE

[1] A. Davidson, "New Wave Phenomena in Series Josephson Junctions," IEEE Tran. Mag., Vol. 17, pp. 103-106, January 1981.

[2] A.K. Jain, K.K. Likharev, J.E. Lukens, and J.E. Sauvageau, "Mutual phase-locking in Josephson junction arrays," Phys. Rep., Vol. 109, pp. 386-414, July 1984.

[3] J.E. Lukens, "Josephson arrays as high frequency sources," in *Superconducting Devices*, Academic Press, 1990, pp. 135-167.

[4] K. Wan, A.K. Jain, and J.E. Lukens, "Submillimeter wave generation using Josephson junctions arrays," Appl. Phys. Lett., Vol. 54, pp. 1805-1807, May 1989.

[5] K. Wan, B. Bi, A.K. Jain, L.A. Fetter, S. Han, W.H. Mallison, and J.E. Lukens, "Refractory submillimeter Josephson effect sources," IEEE Tran. Mag., Vol. 27, pp. 3339-3342, March 1991.

[6] K. Wan, A.K. Jain, L.A. Fetter, W. Zhang, S. Han, and J.E. Lukens, "Development of a rapidly tunable microwave source," Supercond. Sci. Technol., Vol. 4, pp. 647-649, 1991.

[7] K. Wan, "High frequency wave source using Josephson junction arrays," SUNY at Stony Brook, Ph.D. dissertation, 1991.

[8] M. Octavio, C.B. Whan, and C.J. Lobb, "Phase coherence and disorder in Josephson-junction arrays," Appl. Phys. Lett., Vol. 60, pp. 766-768, February 1992.

[9] As a example, an array of 200 Josephson junctions each having $I_c = 4$ mA and $R_s = 0.25$ Ω would produce about 100 μW power into a 50 Ω load at frequencies about 500 GHz. The total bias current would be less than 10 mA for series dc biasing and more than 1 A for parallel dc biasing.

[10] M.B. Ketchen, D. Pearson, A. Kleinsasser, C.-K. Hu, M. Smyth, J. Logan, K. Stawiasz, M. Jaso, K. Petrillo, M. Manny, S. Basavaiah, S. Brodsky, S.B. Kaplan, W.J. Gallagher, and M. Bhushan, "Sub-μm, planarized, Nb-AlO$_x$-Nb Josephson process for 125 mm wafers developed in partnership with Si technology," Appl. Phys. Lett., Vol. 59, pp. 2609-2611, November 1991.

Presented at the Fourth International Symposium on Space Terahertz Technology
March 30–April 1, 1993
UCLA, Los Angeles, California

F

High Power Submillimeter Wave Source using
Series Biased Linear Josephson Effect Array

Siyuan Han, Baokang Bi, Wenxing Zhang, A. H. Worsham, and J. E. Lukens
Department of Physics, SUNY at Stony Brook
Stony Brook, NY 11794, U.S.A.

As millimeter and submillimeter sources, phase-locked array of N Josephson junctions can overcome many shortcomings of the single junction source such as low source impedance, low output power, and large linewidth. In recent years it has been demonstrated that small linear arrays ($N \leq 100$) are capable of delivering several μW power to a load of 10 to 60 Ω in the frequency range of ~ 200 GHz to ~ 500 GHz with linewidth $\Delta f/f < 5 \times 10^{-6}$ [1-4]. For many applications one would like to have higher power and narrower linewidth which can be achieved by increasing the number of junctions deployed in the array since the output power increase as N^2 and linewidth decreases as $1/N^2$ for arrays having $NR_J = R_L$, where R_J and R_L are the junction's shunt resistance and the load resistance, respectively. There are two basic designs for the medium size ($N \sim 10^2$) and large size ($N \sim 10^3$) linear Josephson array: the quasi-lumped array and distributed array [4, 5]. In a quasi-lumped array the distance between two adjacent junctions is λ_0 (wavelength at designed operating frequency). In a distributed array a group of m junctions are closely packed together and the distance between two adjacent groups is λ_0. In both types of array the junctions are embedded in the transmission line structure which provides the long-range high-frequency electromagnetic couplings between the junctions. This coupling is essential to achieve mutual phase locking in the linear array. Compared to the quasi-lumped array, the distributed array requires less space and has smaller internal rf loss (especially as f_0 approaches the superconducting gap frequency of ~ 700 GHz for Nb).

The output rf power coupled to a load R_L from an linear array of N junctions can be written as

$$P_N = \frac{(\gamma N V_c)^2 R_L}{2(N R_J + R_L)^2} \tag{1}$$

when the source impedance matches to the load Eq. (1) becomes

$$P_N = \frac{(\gamma N V_c)^2}{8 R_L} \qquad (2)$$

where $V_c \equiv I_c R_J$ is the characteristic frequency of the junction, I_c is the critical current of the junction. γ depends on the dc bias voltage and is usually less than unity.

We have designed medium size ($N = 500$) distributed array ($m = 10$) oscillators for operation around 400 GHz. Each resistively shunted Nb/AlO/Nb tunnel junction is 5.2 μm^2 in size and has designed parameters of $I_c = 1.4$ mA ($J_c = 27000$ A/cm^2) and $R_J = 0..5$ Ω which give $V_c = 0.7$ mV, $\beta_c \equiv 2\pi V_c R_J C_J / \Phi_0$ $\simeq 0.25$ and $\beta_L \equiv 2\pi I_c L_s / \Phi_0 \simeq 0.8$, where C_J and L_s are the shunt capacitance of the junction and the parasitic inductance associated with the shunt resistor, respectively. Φ_0 is the flux quantum. The total length of the array is about 50 λ_0 (at $\sim$ 400 GHz). The Nb microstrip line is 250 nm thick and 8 μm wide with 670 nm thermally evaporated SiO between the microstrip line and the 340 nm thick Nb ground plane. This gives $Z_0 \simeq 12$ Ω. The designed output power to the 50 Ω load is about 100 μW around 400 GHz.

The Nb/AlO/Nb trilayer films were made at AT&T Bell Laboratory and the arrays were fabricated at IBM using the PARTS process developed by Ketchen et. al [6]. The measured parameters of a typical single junction from wafer #8 are $I_c = 2.5$ mA, $R_J = 0.56$ Ω and $V_c = 1.4$ mV at 4.2 K. This corresponding to a Jc of about 50000 A/cm^2 which is about twice of the designed value. This results in a value of $\beta_c \simeq 0.56$ and $\beta_L \simeq 1.6$ which are quite far away from the designed value and unfavorable for phase-locking. The measured load resistance is 62 Ω.

The output rf power to the load resistor has been measured using the on-chip Josephson junction detectors. The amplitude of the rf current through the detector junction is estimated by comparing the size of the first Shapiro step and the suppression of the critical current to those obtained from the numerical simulations using measured V_c, I_c, and R_J. The estimated output rf power P_{rf} is 45 ± 15 μW using the suppression of I_c and is 50 ± 25 μW using the size of the first Shapiro step. The measured rf power is consistent with $P_{rf} = 65$ μW calculated from Eq. (1) [7]. The measurement of the output power spectrum $P_{rf}(f)$ is currently in progress.

In summary, a linear Josephson effect array oscillator with series dc bias has been designed to deliver rf power of about 100 μW to a 50 Ω load. The measured output power to the 62 Ω load at ~ 400 GHz is 50 μW, lower than designed value., due to the difference between the target critical current and that of the sample.

[1]   K. Wan, A.K. Jain, and J.E. Lukens, "Submillimeter wave generation using Josephson junctions arrays," Appl. Phys. Lett., Vol. 54, pp. 1805-1807, May 1989.

[2]   K. Wan, B. Bi, A.K. Jain, L.A. Fetter, S. Han, W.H. Mallison, and J.E. Lukens, "Refractory submillimeter Josephson effect sources," IEEE Tran. Mag., Vol. 27, pp. 3339-3342, March 1991.

[3]   Baokng Bi, Siyuan Han, and J.E. Lukens, "Radiation Linewidth of Phase Locked Distributed Array in the Submillimeter Wave Range", to be published in Appl. Phys. Lett.

[4]   Siyuan Han, A.H. Worsham, and J.E. Lukens, "Complete Phase-Locking in a One-Dimensional Series Biased Josephson-Junction Array", to be published in the Proceedings of 1992 Applied Superconductivity Conference.

[5]   Baokang Bi, Siyuan Han, and J.E. Lukens, "Distributed Josephson Junction Arrays as Local Oscillators", to be published in the Proceedings of 1992 Applied Superconductivity Conference.

[6]   M.B. Ketchen, D. Pearson, A. Kleinsasser, C.-K. Hu, M. Smyth, J. Logan, K. Stawiasz, M. Jaso, K. Petrillo, M. Manny, S. Basavaiah, S. Brodsky, S.B. Kaplan, W.J. Gallagher, and M. Bhushan, "Sub-μm, planarized, Nb-AlO$_x$-Nb Josephson process for 125 mm wafers developed in partnership with Si technology," Appl. Phys. Lett., Vol. 59, pp. 2609-2611, November 1991.

[7]   In deriving Eq. (1) it is assumed the junctions can be approximated well by the RSJ model. However, this condition is not met by the junctions used in this work. Thus Eq. (1) can be used only to give a rough estimate of P_{rf}.

HIGH POWER SUBMILLIMETER RADIATION FROM DISTRIBUTED 1D JOSEPHSON JUNCTION ARRAYS

Siyuan Han, Baokang Bi, Wenxing Zhang, and J. E. Lukens

Department of Physics, SUNY at Stony Brook
Stony Brook, NY 11794, USA 516/632-8076

For many submillimeter wave (SMW) frequency applications it is essential to have a compact source capable of delivering rf power in the range of $10 - 100$ μW to a load around 50 Ω. The highest rf power measured from a Josephson effect oscillator was 7 μW at ~ 300 GHz reported by Wan et. al [1-4]. Recently, we have obtained rf power of greater than 50 μW coupled to ~ 60 Ω load around 400 GHz from distributed linear Josephson arrays [4] of 500 junctions with series dc biasing.

The rf power coupled to a load R_L from an completely phase-locked linear array of N Josephson junctions can be written as

$$P_N = \kappa(\gamma N V_c)^2 R_L/[2 (N R_J + R_L)^2] \qquad (1)$$

Here, R_J is the normal state resistance of each junction, $V_c \equiv I_c R_J$ is the characteristic voltage of the junction and I_c is the critical current. γ and κ are factors of order unity which depend on the junction parameters and array design. In general γ and κ must be obtained by computer simulation.

The distributed array (shown in Fig. 1) has 500 resistively shunted junctions placed along a microstrip transmission line. Ten junctions are grouped into a lump in which two adjacent junctions are separated by 10 μm. Adjacent lumps are separated by one wavelength at the designed operating frequency. Load resistors and Josephson junction detectors are placed at both ends of the array. The arrays were fabricated at IBM using PARTS technology [5] with high critical current density ($J_c \approx 30 - 50$ kA/cm^2) Nb/AlO$_x$/Nb trilayers made at AT&T Bell Laboratory. $700 - 800$ nm of thermally evaporated SiO was used as the dielectric between the Nb microstrip and the 300 nm Nb ground plane. Each load resistor and detector junction has independent dc bias leads which allows us to make four terminal measurement to determine their parameters. R_J is measured by suppressing the junction's critical current with a magnetic field. The capacitance of the 6 μm^2 junctions is estimated to be ~ 290 fF including parasitic capacitance. The parasitic inductance L associated with the external shunt resistor is 0.18 pH estimated from the physical dimensions of the shunt.

The coherent rf current generated by the array is measured by the detector junctions placed after the loads. The magnitude of the n=1 Shapiro step [6] is used to obtain the amplitude of the coherent rf current I_{rf} through the junction and the load by fitting the measured IV curve to that of numerical simulations using measured junction parameters. For numerical simulations, the detector junction has to be described by the Resistively-Inductively and Capacitively Shunted Junction (RICSJ) model due to the rather large value of LI_c [7].

Five samples have been completed and tested for SMW generation. All of them have > 20 μW coupled to a ~ 60 Ω load around 400 GHz. The dc IV curves of a 500 junction array and its detector junction from sample W11D8 are shown in Fig. 2. The array has an average critical current $I_c \approx 3.2$ mA and an average $R_J \approx 0.4$ Ω. The detector junction has $I_c \approx 3.45$ mA, $R_J \approx 0.4$ Ω, Fig. 3 shows the measured IV curve around the n=1 Shapiro step at 1.9 K and that of the simulation using the measured parameters above and $I_{rf} = 1.22$ mA. The measured load resistance is 68 Ω for this sample thus giving rf power $I_{rf}^2 R_L/2 \simeq 50$ μW at 400 GHz. The size of the n=1 Shapiro step of sample W8F5 as a function of array's oscillation frequency is displayed in Fig. 4. Note that the array oscillator generated usable rf power (> 1 μW) into ~ 60 Ω over a fairly wide frequency range ($300 - 450$ GHz). More than 10 μW rf power at 500 GHz has been obtained from sample W11D8.

In summary, series dc biased 500 junction distributed Josephson junction arrays have been designed, fabricated and tested. The measured maximum coherent rf power coupled to a 60 Ω load at

400 GHz is greater than 50 μW. Coherent rf power above 10 μW has also been measured at 500 GHz from the array oscillator.

[1] K. Wan, A.K. Jain, and J.E. Lukens, Appl. Phys. Lett., **54**, 1805 (1989).
[2] S.P. Benz and C.J. Burroughs, Appl. Phys. Lett., **58**, 2162 (1991).
[3] Y.M. Zhang, D. Winkler, and T. Claeson, IEEE Trans. Appl. Supercon., **3**, 2520 (1993). V.P. Koshelets, A.V. Shchukin, S.V. Shitov, *ibid.* **3**, 2524 (1993).
[4] B. Bi, S. Han, and J.E. Lukens, IEEE Trans. Supercon., **3**, 2303 (1993). B. Bi, S. Han, and J.E. Lukens, Appl. Phys. Lett., **62**, 2745 (1993).
[5] M.B. Ketchen, D. Pearson, A. Kleinsasser, C.-K. Hu, M. Smyth, J. Logan, K. Stawiasz, M. Jaso, K. Petrillo, M. Manny, S. Basavaiah, S. Brodsky, S.B. Kaplan, W.J. Gallagher, and M. Bhushan, Appl. Phys. Lett., **59**, 2609 (1991).
[6] S. Shapiro, Phys. Rev. Lett., **11**, 80 (1963).
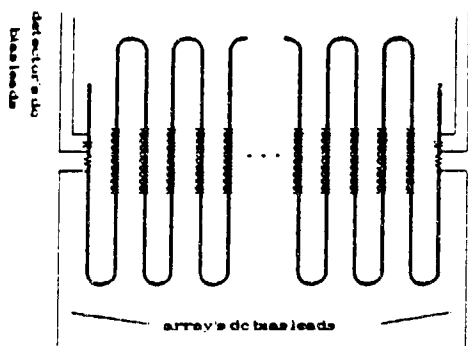[7] S. Han, A.H. Worsham, and J.E. Lukens, IEEE Trans. Appl. Supercon., **3**, 2489 (1993).

Fig. 1 Schematics of 500 junction series biased distributed array.
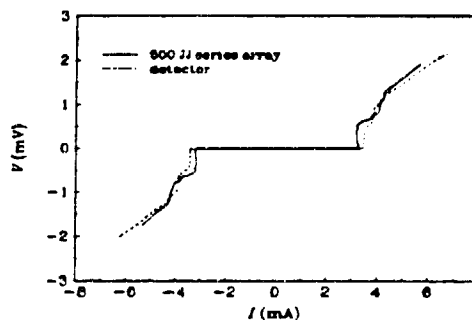

Fig. 2 dc IV curves of the array and the detector junction. Array's voltage has been divided by 500 (sample W11D8).
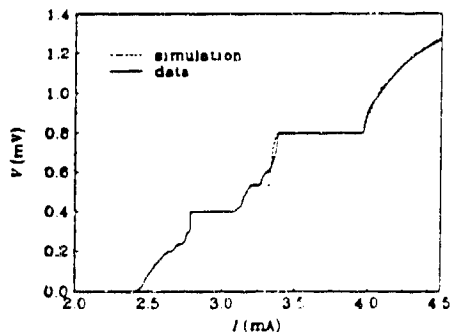

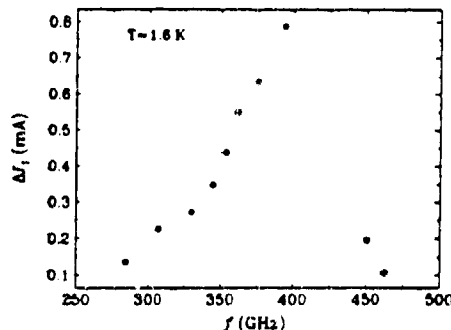Fig. 3 The data and simulation of detector's IV curve with array on (sample W11D8).

Fig. 4 Measured size of n=1 Shapiro step vs. frequency (sample W8F5).

Demonstration of Josephson Effect Submillimeter Wave Sources with Increased Power

Siyuan Han, Baokang Bi, Wenxing Zhang, and J. E. Lukens
Department of Physics, University at Stony Brook
Stony Brook, NY 11794

ABSTRACT

A submillimeter wave source based on a new design using Josephson junction arrays has been developed and tested. The maximum rf power, delivered to a 68 Ω load and detected on-chip, was $47\,\mu W$ at 394 GHz. Significant power was detected at a number of frequencies from 300 GHz to 500 GHz where the power was $10\,\mu W$. The observed power at the designed operating frequency near 400 GHz is consistent with all 500 junctions in the series biased array delivering current in-phase to the loads. This is in agreement with simulations of smaller arrays of the same design. The linewidth, inferred from the measured resistance at the point of maximum power, with $T = 4.2\,K$, is less than 1 MHz. The minimum inferred linewidth near 400 GHz, at somewhat lower power, is about 100 kHz.

Many submillimeter wave (SMW) frequency applications, such as radio astronomy and high speed communication, require a compact SMW source capable of delivering rf power in the range of $10 - 100\,\mu W$. For frequencies above 300 GHz, the lack of compact sources is particularly serious requiring increasingly inefficient multiplication of millimeter wave sources. Lately there has been a substantial effort to develop Josephson effect sources, which can work to at least 1 THz [1], for applications in the SMW [2-4]. The most promising results, recently obtained, have come from three types of sources: long single junctions flux flow oscillators [2], various types of two dimensional arrays of small junctions [3] and one dimensional (1D) small junction arrays [4], discussed here. In general a power of about $1\,\mu W$ is obtained from these sources, although in many cases the source impedance is less than $1\,\Omega$. The highest rf power previously reported from a Josephson effect oscillator has been $7\,\mu W$ at ~ 300 GHz by Wan et. al [4] using a 1D array. Here we report results from an improved design for Josephson SMW sources—distributed linear arrays of 500 Josephson junctions with series dc biasing—generating an rf power of $47\,\mu W$ around 394 GHz and $10\,\mu W$ at 500 GHz into an on-chip load of $68\,\Omega$.

Small resistively shunted junctions (RSJ), described by the RSJ model [5], are characterized by a critical current I_c and a shunt resistance R_J, and generate a peak rf voltage $V_{rf} = \gamma V_c$ ($V_c \equiv I_c R_J$) with a source impedance Z_s at the Josephson frequency, $f_J = 483.6$ GHz/mV. For bias voltage $V > V_c$, $\gamma \rightarrow 1$ and $Z_s \rightarrow R_J$. The junctions are placed in a superconducting microstrip and interact via the rf current I_{rf} generated in the microstrip by the Josephson oscillations. For properly designed arrays [6] the rf voltages across the junctions can be made to add in series. This will be true independent of the relative polarities, along the microstrip, of the junctions' biases, i. e. the dc voltage can sum to NV_c (series bias) or to zero (parallel bias). The power from such an array (see Fig. 1) is then just,

$$P_N = \kappa \frac{(\gamma N V_c)^2 R_L}{2(N R_J + R_L)^2} .$$ (1)

Here N is the number of rf series elements in the array, and R_L is the load impedance seen by the array. $\kappa = 1$ is the ideal case, but is in general somewhat less than unity due to losses in the coupling structure or imperfect phase alignment of the junctions. For 1D arrays (Fig. 1a-c), N is just the number of junctions in the array. For 2D arrays (Fig. 1d) of the types so far reported, the rf current flow is ideally along rows of junctions,

with the phase of the rf current transverse to this flow (i.e. across a column) being constant. Equation 1 can then be applied to 2D arrays as well if one replaces N by N_s, the number of series elements (i.e. columns) in the array and R_J by R_{J_s}, the resistance of a series element. The power from an array matched to the load, i.e. with $N_s r_{J_s} = R_L$, is $P_N \simeq (N_s V_c)^2 / 8 R_L$, and can in principle be increased just by increasing N_s while keeping $N R_J$ and V_c constant. This implies that $I_{cs} \propto N_s$ and $P_N \simeq R_L I_{cs}^2 / 8$.

Increasing the source power, therefore, requires increasing I_{cs}, adding together enough series elements to match the array impedance to the load and maintaining phase coherence throughout the array. In practice, there are two essential limitations to this increase. First, when I_{cs} becomes greater than several milliamps, there exists the potential for flux flow instabilities which would dissipate power internally in both single junctions and in the columns of 2D arrays. It is not yet clear whether there is an advantage to 1D or 2D arrays for maximizing I_{cs} while maintaining phase stability. The second problem, common to both 1D and 2D arrays, is that when the length of the array becomes an appreciable fraction of the wavelength, care must be taken to maintain the proper phase relationship between the junction oscillations and the rf current throughout the array. This is required so that all junctions phase lock in a stable manner and provide current to the load with the same phase. Especially for the SMW source, this problem must be solved to permit the use of enough junctions to obtain power levels much above a microwatt. It is this second problem which we address in this paper.

Fully coherent 1D arrays have been demonstrated using both a lumped circuit design (Fig. 1a), where the array length $L < \lambda/10$ [6] (λ is the wavelength in the microstrip coupling the junctions), or the so-called quasi-lumped design where the junctions' spacing is λ [4]. The number of junctions in both designs is severely limited in the SMW. A maximum of about $N = 10$ can be used in the SMW for lumped arrays made with standard fabrication technologies. For quasi-lumped arrays, losses in the microstrip coupling the junctions as well as the larger array size are limitations. Much denser packing can be achieved if the junctions can be distributed along the microstrip for a significant fraction of λ. Figure 1c shows such a structure where groups of M junctions are placed at intervals of λ or $\lambda/2$ along the microstrip. Our computer simulation shows that for same N and M arrays with $\lambda/2$ inter-lump distance have a wider tuning range.

Distributed arrays (shown in Fig. 2) of 500 junctions have been designed,

fabricated, and tested for SMW generation. Resistively shunted Nb/AlO$_x$/Nb tunnel junctions are placed in groups of ten junctions ($M = 10$) with adjacent junctions in the group separated by 10 μm. Adjacent groups are separated by one wavelength at the designed primary operating frequency of ~ 390 GHz. Load resistors and Josephson junction detectors to measure the rf currents are placed at both ends of the array. The arrays were fabricated at IBM using Planarized All-Refractory Technology for Superconductivity [7] with high critical current density ($J_c \approx 40 - 60$ kA/cm^2) Nb/AlO$_x$/Nb trilayers made at AT&T Bell Laboratory. 700 nm of thermally evaporated SiO was used as the dielectric between the Nb microstrip and the 300 nm Nb ground plane, which was placed on top of the array. Each load resistor and detector junction has independent dc bias leads allowing their parameters to be determined using four terminal measurements. R_J is measured by suppressing the junctions' critical current with a magnetic field. The capacitance of the 6 μm^2 junctions, including parasitic capacitance, is estimated from the geometry and the specific capacitance of 46 fF/μm^2 to be ~ 290 fF . The parasitic inductance L associated with the external shunt resistor is 0.18 pH estimated from the physical dimensions of the shunt. The junctions in the array are biased in series using a common dc current. This requires a higher degree of junction uniformity, but is important for larger arrays. For example, the arrays studied here would have required a bias current of over 2 A for parallel bias instead of the 5 mA actually used.

The coherent rf current generated by the array is measured by the detector junctions placed after the lumped resistor loads. The magnitude of the $n=1$ Shapiro step [8] is used to obtain the amplitude of the coherent rf current I_{rf} through the detector junction and the load resistor by fitting the measured IV curve to that of numerical simulations using measured junction parameters. For numerical simulations, the detector junction has to be described by the Resistively-Inductively and Capacitively Shunted Junction model [9] due to the rather large value of LI_c.

Five samples have been completed and tested for SMW generation. All delivered more than 20 μW of rf power near 394 GHz to loads of about 65 Ω. For sample W11D8, the average critical current of the junctions in the array is $I_c = 3.2$ mA and the average junction resistance is $R_J = 0.38 \Omega$. The detector junctions have an $I_c \simeq 3.5$ mA, and a $R_J = 0.38 \Omega$. The maximum power from the array occurs at 394 GHz, however, significant power is available at a number of frequencies in the 300 GHz to 500 GHz range

with $10\,\mu$W of power delivered to the loads at 500 GHz. Figure 3 shows the measured IV curve of a detector around the $n=1$ Shapiro step with the array operating at 394 GHz and $T = 1.9$ K. This is compared with that of the detector simulation using the measured junction parameters and an rf current amplitude from the array of $I_{rf} = 1.18$ mA. The measured total load resistance is $68\,\Omega$ for this sample giving an rf power, $I_{rf}^2 R_L/2 \simeq 47\,\mu$W at 394 GHz. Since the total array resistance is $190\,\Omega$ (the actual junctions shunt resistors were somewhat greater than the design values) the maximum available power from this array (into a $190\,\Omega$ load) would be $64\,\mu$W at 394 GHz.

The measured power of $\sim 50\,\mu$W at 394 GHz compares reasonably with the value of $96\,\mu$W from Eq. 1, assuming perfect alignment of the junctions' phases and no transmission line losses (i.e. $\kappa = 1$). However, κ is in general always less than unity due to imperfect phase alignment and the losses in the coupling structure (in our case, a microstrip transmission line). The measured value of $\kappa = 47/96 \simeq 0.49$ at 394 GHz can be entirely accounted for by a surface resistance of $7\,m\Omega$, assuming nearly perfect phase alignment. Our computer simulations of an array with $N = 100$ but otherwise identical in structure to that measured indeed show a negligible phase spread among the junctions. Although the surface resistance of the actual sample has not been measured, the value inferred from the rf power measurement ($7\,m\Omega$) is consistent with the measured surface resistance at about 400 GHz in Nb/SiO/Nb microstrip resonators [10] and compares favorably to that obtained by Cucolo $et\ al.$ [11].

The second major advantage of the phase-locked array source is that the radiation linewidth can be substantially reduced since the phase-locking suppresses the frequency modulation of the array due to the random noise sources associated with the junction shunt resistors. The linewidth of a series array of N identical Josephson junctions is approximately given by [6, 12, 13]:

$$\Delta f \simeq \left(\frac{2\pi}{\Phi_0}\right)^2 \left(\frac{k_B T}{\pi R_J}\right) \frac{R_d^2}{N}\left[1 + 2\alpha^2 x \coth(x)\right], \qquad x \equiv \frac{hf}{2k_B T}. \qquad (2)$$

where k_B is the Boltzmann constant, h is Planck's constant, Φ_0 is the magnetic flux quantum, R_d is the dynamic resistance of an independent junction, and $\alpha \simeq 0.42$ is the down conversion coefficient. Equation 2 requires some modification in distributed arrays, since the strength of the locking can depend on the position of the junction. However, direct measurements of the linewidth [13] in a small array consisting of two groups of

junctions separated by $\lambda/2$ show that, within a factor of 2 to 3, Eq. 2 provides a reliable estimate of Δf. Using values of R_d and R_J as the average over the array, the implied linewidth at 394 GHz is about 730 kHz at $T = 4.2$ K decreasing to 475 kHz at 1.6 K, where $x \simeq 5.9$, so zero point fluctuations dominate. The value of R_d varies with bias current giving a minimum implied linewidth of about 100 kHz at $T = 4.2$ K near 375 GHz but with a somewhat lower power level.

In summary, 500 junction Josephson effect arrays using dc series bias and a distributed junction layout have been designed, fabricated and tested. The measured maximum coherent rf power coupled to a 68 Ω load at 394 GHz is 47 μW, implying an available power of 64 μW. An rf power of 10 μW has also been measured at 500 GHz from the array oscillator. At 4.2 K the linewidth near 400 GHz, calculated from Eq. (2) using the measured array parameters, is less than 730 kHz.

REFERENCES

[1]   R.P. Robertazzi and R.A. Buhrman, IEEE Trans. Mag. **MAG-25**, 1384 (1989).

[2]   Y.M. Zhang, D. Winkler, and T. Claeson, Appl. Phys. Lett. **62**, 3195 (1993). V.P. Koshelets, A.V. Shchukin, S.V. Shitov, IEEE Trans. Appl. Supercon. **3**, 2524 (1993).

[3]   S.P. Benz and C.J. Burroughs, Appl. Phys. Lett. **58**, 2162 (1991). J.S. Martens, A. Pance, K. Char, L. Lee, S. Whiteley, and V.M. Hietala, *ibid*. **63**, 1681 (1993).

[4]   K. Wan, A.K. Jain, and J.E. Lukens, Appl. Phys. Lett. **54**, 1805 (1989).

[5]   D.E. McCumber, J. Appl. Phys. **39**, 2113 (1968). W.C. Stewart, Appl. Phys. Lett. **12**, 277 (1968).

[6]   A.K. Jain, K.K. Likharev, J.E. Lukens, and J.E. Sauvageau, Phys. Rep. **109**, 309 (1984). J.E. Lukens, in *Superconducting Devices*, edited by S.T. Ruggiero and D.A. Rudman (Academic, San Diego, 1991), p. 135.

[7]   M.B. Ketchen, D. Pearson, A. Kleinsasser, C.-K. Hu, M. Smyth, J. Logan, K. Stawiasz, M. Jaso, K. Petrillo, M. Manny, S. Basavaiah, S. Brodsky, S.B. Kaplan, W.J. Gallagher, and M. Bhushan, Appl. Phys. Lett. **59**, 2609 (1991). R.E. Miller, W.H. Mallison, A.W. Kleinsasser, K.A. Delin, and E.M. Macedo, Appl. Phys. Lett. **63**, 1423 (1993).

[8]   S. Shapiro, Phys. Rev. Lett. **11**, 80 (1963).

[9]   S. Han, A.H. Worsham, and J.E. Lukens, IEEE Trans. Appl. Supercon. **3**, 2489 (1993).

[10] B. Bi, K. Wan, W. Zhang, S. Han, and J.E. Lukens, IEEE Trans. Appl. Supercon. **1**, 145 (1991).

[11] A.N. Cucolo, S. Pace, R. Vaglio, V. Lacquaniti, and G. Marullo, IEEE Trans. Magn. **MAG-17**, 812 (1981).

[12] K.K. Likharev and V.K. Semenov, JETP Lett. **15**, 442 (1972).

[13] B. Bi, S. Han, and J.E. Lukens, Appl. Phys. Lett. **62**, 2745 (1993).

FIGURE CAPTIONS

Fig. 1. Some typical structures for Josephson junction arrays: (a) 1D Lumped array. (b) Quasi-lumped array. (c) Distributed array. (d) 2D array. λ is the wavelength at the primary operating frequency; I_b is the dc bias current.

Fig. 2. Schematics of the $N = 500$, $M = 10$ serial biased 1D distributed Josephson junction array for SMW generation.

Fig. 3. The measured IV curve (solid line) around the $n = 1$ Shapiro step at $798\,\mu$V of the detector junction on sample W11D8 under 394 GHz irradiation from the array and the IV curve obtained from computer simulation (solid circles) using RICSJ model. The parameters used for the simulation are $I_c = 3.47\,$mA, $C = 294\,$fF, $L = 0.178\,$pH. $R_J = 0.377\,\Omega$, and $I_{rf} = 1.18\,$mA. This rf current amplitude corresponds to a power of $47\,\mu$W in the load of $68\,\Omega$.

(a)

(b)

(c)

(d)

load resistor

array's bias leads

detector's
bias leads
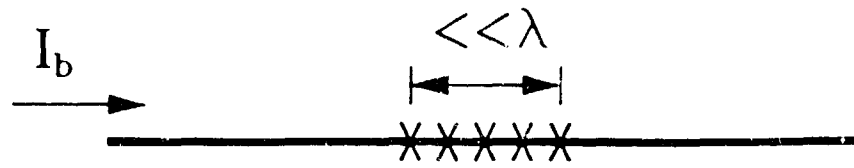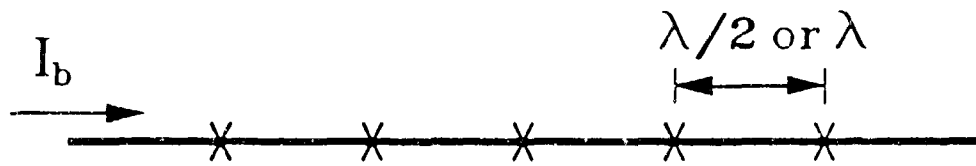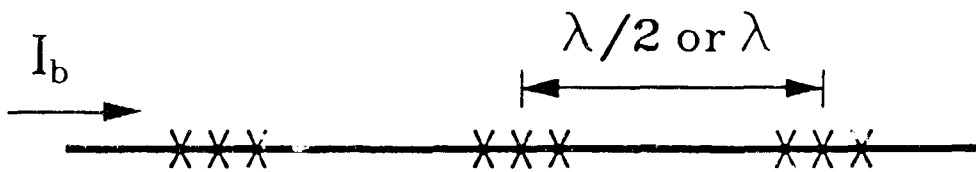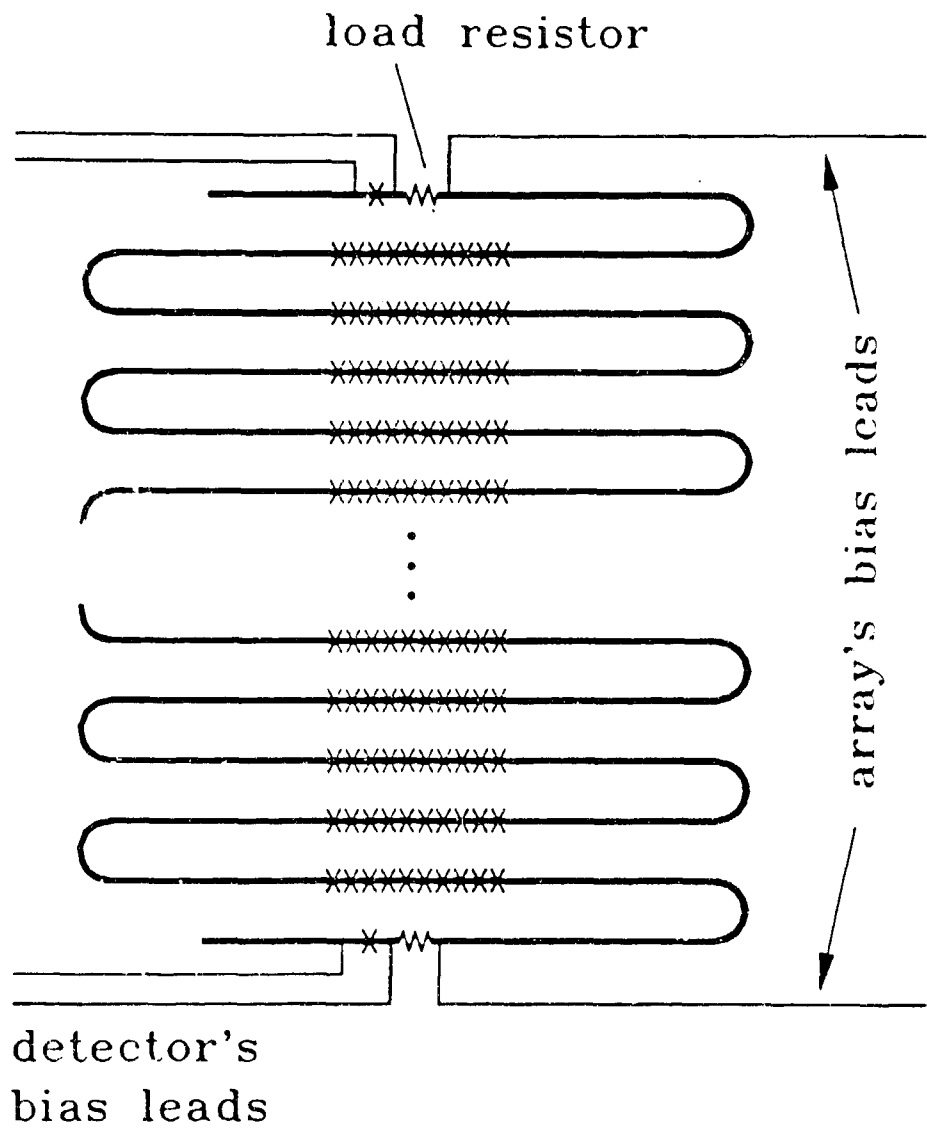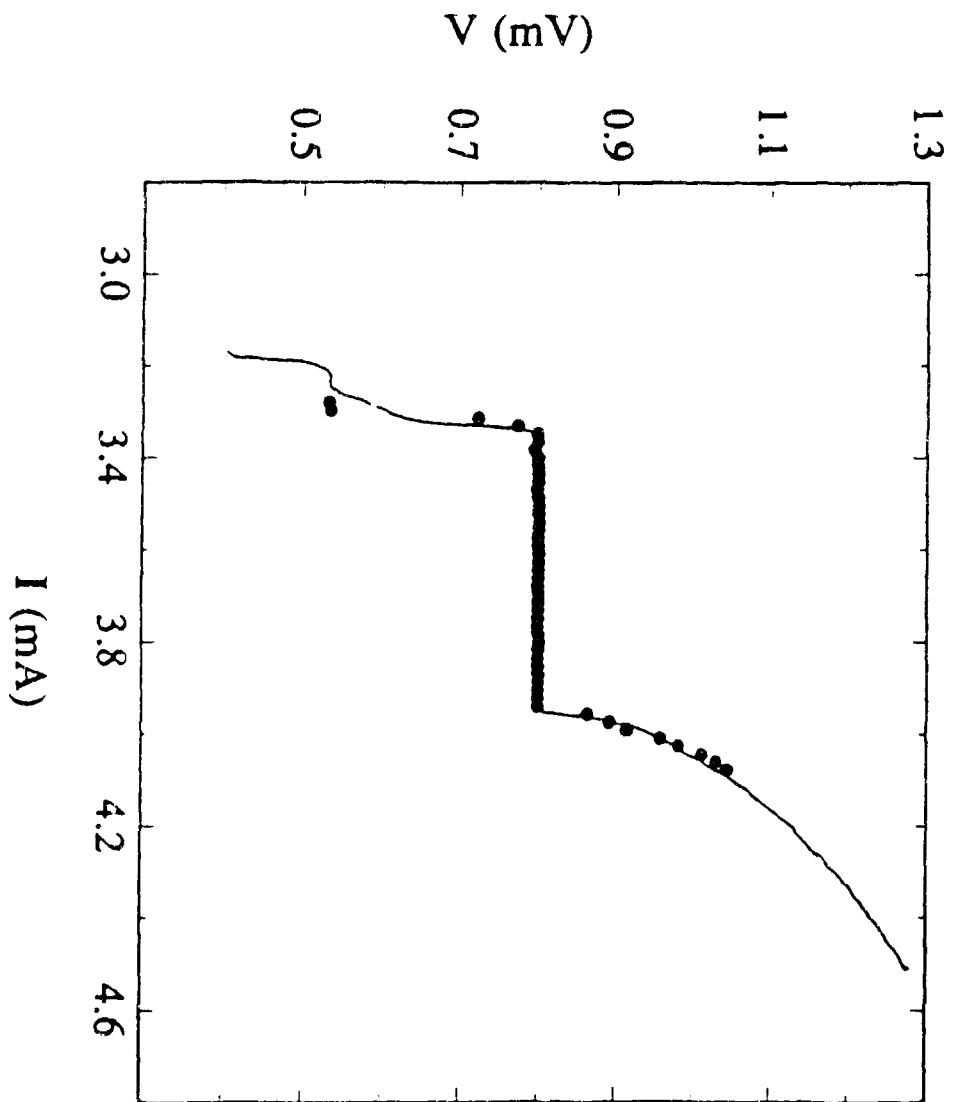
DISTRIBUTION LIST

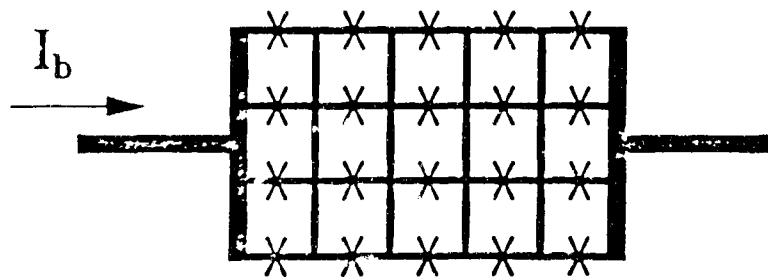| addresses	number of copies
MR JOHN P TURTLE ROME LABORATORY/ERAA 31 GRENIER STREET HANSCOM AFB MA 01731-3010	10
MR JAMES LUKENS STATE UNIVERSITY OF NEW YORK DEPARTMENT OF PHYSICS STONY BROOK NY 11794	5
RL/SUL TECHNICAL LIBRARY 26 ELECTRONIC PKY GRIFFISS AFB NY 13441-4514	1
ADMINISTRATOR DEFENSE TECHNICAL INFO CENTER DTIC-FDAC CAMERON STATION BUILDING 5 ALEXANDRIA VA 22304-6145	2
BALLISTIC MISSILE DEFENSE ORGANIZATION 7100 DEFENSE PENTAGON WASH DC 20301-7100	2
DR. ANDREW SMITH APPLIED TECHNOLOGY DIVISION TRW SPACE AND TECHNOLOGY GROUP ONE SPACE PARK REDONDO BEACH, CA 90278	1
DR. ROBERT A. BUHRMAN DEPT OF APPLIED & ENGINEERING PHY. CORNELL UNIVERSITY ITHACA, NY 14853	1
DR. JOHN X. PRZYBYSZ WESTINGHOUSE SCIENCE & TECH. CEN. 1310 BEULAH ROAD PITTSBURG, PA 15235	1

DR. RICHARD RALSTON   1
ANALOG DEVICE TECHNOLOGY GROUP
MIT LINCOLN LABORATORY
LEXINGTON, MA 02173-0073

                                                       1

DR. HAROLD WEINSTOCK
AFOSR/NE
BOLLING AFB, DC 20332-6448

PROF. MALCOLM BEASLEY   1
DEPT. OF APPLIED PHYSICS
EDWARD L. GINZTON LABORATORY
STANFORD UNIVERSITY
STANFORD, CA 94305

DR. TED VAN DUZER   1
DEPT OF ELECTRONICS ENGINEERING
  AND COMPUTER SCIENCE
UNIVERSITY OF CALIFORNIA
BERKELEY, CA 94720

DR. JAMES LUKENS   1
DEPT. OF PHYSICS
STATE UNIVERSITY OF NEW YORK
STONY BROOK, NY 11794-3800

DR. ELIE K. TRACK   1
HYPRES INC.
500 EXECUTIVE BLVD.
ELMSFORD, NY 10523

DR. MARTIN NISENOFF   1
CODE 6854
NAVAL RESEARCH LABORATORY
WASHINGTON, DC 20375-5000

PROF. DAVID RUTLEDGE   1
CALIFORNIA INSTITUTE OF TECHNOLOGY
MAIL CODE 116-81
PASADENA, CA 91125

DR. STANLEY REIBLE   1
MICRILOR INC.
17 LAKESIDE OFFICE PARK
NORTH AVENUE
WAKEFIELD, MA 01880

AFIWC/MSO   1
102 HALL BLVD STE 315
SAN ANTONIO TX 78243-7016

DR. HENRY LEDUC   1
MS 122-123
JET PROPULSION LABORATORY
4800 OAK GROVE DR.
PASADENA, CA   91109

PROF. THOMAS PHILLIPS   1
MS 320-47
CALIFORNIA INSTITUTE OF TECHNOLOGY
PASADENA, CA   91125

PROF. ROBERT MATTAUCH   1
DEPT. OF ELECTRICAL ENGINEERING
UNIVERSITY OF VIRGINIA
CHARLOTTESVILLE, VA   22901

DR. FRANK PATTON   1
DARPA/DSO
3701 NORTH FAIRFAX DRIVE
ARLINGTON, VA   22203-1714

DR. WILLIAM MCGRATH   1
MS 168-314
JET PROPULSION LABORATORY
4800 OAK GROVE DR.
PASADENA, CA   91109

PROF. NEAL ERICKSON   1
DEPT. OF PHYSICS AND ASTRONOMY
UNIV. OF MASSACHUSETTS
AMHERST, MA   01002

PROF. PAUL RICHARDS   1
DEPT. OF PHYSICS
UNIVERSITY OF CALIFORNIA
BERKELEY, CA   94720

PROF. MARC FELDMAN   1
DEPT. OF ELECTRICAL ENGINEERING
UNIVERSITY OF ROCHESTER
ROCHESTER, NY   14623

DR. A. P. KERR   1
NATIONAL RADIO ASTRONOMY OBSER.
2015 IVY RD.
CHARLOTTESVILLE, VA   22903-1797

DR. ROBIN HARVEY   1
HUGHES RESEARCH LABORATORY
3011 S. MALIBU CANYON RD.
MALIBU, CA   90265

DR. FERNAND D. BEDARD   1
NSA ATTN. R53
9800 SAVAGE RD.
FORT GEORGE G. MEADE, VA 20755-6000

DEPARTMENT OF DEFENSE   1
BMDO/TRI
CRYSTAL SQUARE ANNEX
WASHINGTON DC 20301-7100

DR. JAMES W. MINK, DIRECTOR   1
ELECTRONICS DIVISION
U.S ARMY RESEARCH OFFICE
P.O. BOX 12211
RESEARCH TRIANGLE PARK, NC 27709

PROF. GABRIEL REBEIZ   1
ELECT. ENG. AND COMPUTER SCIENCE
    DEPARTMENT
UNIVERSITY OF MICHIGAN
ANN ARBOR, MI 48102-2122

PROF. MICHAEL WENGLER   1
DEPARTMENT OF ELECTRICAL ENG.
UNIVERSITY OF ROCHESTER
ROCHESTER, NY 14627

DR. RICHARD WITHERS   1
CONDUCTUS, INC.
969 WEST MAUDE AVE
SUNNYVALE, CA 94056

DR. CHARLES E. BYVIK   1
W. J. SCHAFER ASSOC.
1901 N. FORT MYER DRIVE
SUITE 800
ARLINGTON, VA 22209

DR. RICHARD HARRIS
NIST
DEPT. OF COMMERCE
325 BROADWAY
BOULDER, CO 80303

1

DL-5

MISSION

OF

ROME LABORATORY

Mission. The mission of Rome Laboratory is to advance the science and technologies of command, control, communications and intelligence and to transition them into systems to meet customer needs. To achieve this, Rome Lab:

   a. Conducts vigorous research, development and test programs in all applicable technologies;

   b. Transitions technology to current and future systems to improve operational capability, readiness, and supportability;

   c. Provides a full range of technical support to Air Force Materiel Command product centers and other Air Force organizations;

   d. Promotes transfer of technology to the private sector;

   e. Maintains leading edge technological expertise in the areas of surveillance, communications, command and control, intelligence, reliability science, electro-magnetic technology, photonics, signal processing, and computational science.

The thrust areas of technical competence include: Surveillance, Communications, Command and Control, Intelligence, Signal Processing, Computer Science and Technology, Electromagnetic Technology, Photonics and Reliability Sciences.